Boundary conditions on quasi-Stokes velocities in parameterisations

Peter D. Killworth

Southampton Oceanography Centre, Empress Dock, Southampton SO14 3ZH

ABSTRACT

This paper examines the implications for eddy parameterisations of expressing them in terms of the quasi-Stokes velocity. Another definition of low-passed time averaged mean density (the modified mean) must be used, which is the inversion of the mean depth of a given isopycnal. This definition naturally yields lighter (denser) fluid at the surface (floor) than the Eulerian mean, since fluid with these densities occasionally occurs at these locations. The difference between the two means is second-order in perturbation amplitude, and so small, in the fluid interior (where formulae to connect the two exist). Near horizontal boundaries, the differences become first order, and so more severe. Existing formulae for quasi-Stokes velocities and streamfunction also break down here. It is shown that the low-passed time mean potential energy in a closed box is incorrectly computed from modified mean density, the error term involving averaged quadratic variability.

The layer in which the largest differences occur between the two mean densities is the vertical excursion of a mean isopycnal across a deformation radius, at most about 20 m thick. Most climate models would have difficulty in resolving such a layer. We show here that extant parameterisations appear to reproduce the Eulerian, and not modified mean, density field and so do not yield a narrow layer at surface and floor either. Both these features make the quasi-Stokes streamfunction appear to be non-zero right up to rigid boundaries. It is thus unclear whether more accurate results would be obtained by leaving the streamfunction non-zero on the boundary – which is smooth and resolvable – or by permitting a delta-function in the horizontal quasi-Stokes velocity by forcing the streamfunction to become zero exactly at the boundary (which it formally must be), but at the cost of small and unresolvable features in the solution.

This paper then uses linear stability theory and diagnosed values from eddy-resolving models, to ask the question: *if climate models cannot or do not resolve the difference between Eulerian and modified mean density, what are the relevant surface and floor quasi-Stokes streamfunction conditions, and what are their effects on the density fields?*

The linear Eady problem is used as a special case to investigate this, since terms can be explicitly computed. A variety of eddy parameterisations is employed for a channel problem, and

the time-mean density is compared with that from an eddy-resolving calculation. Curiously, although most of the parameterisations employed are formally valid only in terms of the modified density, they all reproduce only the Eulerian mean density successfully. This is despite the existence of (numerical) delta-functions near the surface. The parameterisations were only successful if the vertical component of the quasi-Stokes velocity was required to vanish at top and bottom. A simple parameterisation of Eulerian density fluxes was, however, just as accurate and avoids delta-function behaviour completely.

1. Introduction

During the last decade, oceanographers have realised that coarse-resolution ocean models cannot adequately represent the ocean in a coupled climate model without some modifications to represent eddies. There has been a variety of schemes suggested to include eddy effects. These schemes divide into two categories. The first, which we shall be examining here, involves adding terms to represent the additional thickness flux by baroclinic eddies (Gent and McWilliams, 1990; Greatbatch and Lamb, 1990; Gent et al, 1995; Visbeck et al, 1997; Treguier et al, 1997; Killworth, 1997, 1998; Greatbatch, 1998). The second (Neptune) involves a representation of the statistical properties of eddies on the mean flow (Eby and Holloway, 1994; Merryfield and Holloway, 1997), and is not discussed here.

The effects of thickness flux can be written in a variety of ways which should formally be identical. One way is always a simple average of the product of two varying quantities. If isopycnal co-ordinates are employed, this term is the divergence of $\overline{\mathbf{u}'h'}$, where $\mathbf{u}$ is the horizontal velocity and h the thickness between two neighbouring isopycnals (proportional to z_ρ, where z is the height of an isopycnal and ρ the density). Analytically,

$$\overline{h}_t + \nabla_H \cdot (\overline{\mathbf{u}}\,\overline{h} + \overline{\mathbf{u}'h'}) = \overline{h}_t + \nabla_H \cdot \{(\overline{\mathbf{u}} + \mathbf{u}^*)\overline{h}\} = 0 \qquad (1.1)$$

where the average is a low-pass time average on a density surface, and the suffix H denotes purely horizontal terms. In (1.1) the thickness flux is written as an additional, horizontal 'bolus' velocity $\mathbf{u}^* \equiv \overline{\mathbf{u}'h'}/\overline{h}$, which advects the mean thickness. An eddy parameterisation in an isopycnic model would supply a form for this term, which would vanish on vertical sidewalls.

If z-co-ordinates are employed, however, the situation is somewhat more awkward. The rough equivalent of thickness flux divergence becomes the divergence of $\overline{\mathbf{u}'\rho'}$:

$$\overline{\rho}_t + \nabla \cdot (\overline{\mathbf{u}}\,\overline{\rho}) + \nabla \cdot (\overline{\mathbf{u}'\rho'}) = 0 \qquad (1.2)$$

where averages are now Eulerian, and the divergence is fully three-dimensional. While $\nabla \cdot (\overline{\mathbf{u}'\rho'})$ (a scalar) can be parameterised, the more usual approach is to seek parameterisations for some equivalent of the bolus velocity.[1] This turns out to be neither easy nor straightforward due to a

[1] One such parameterisation is suggested and tested later; in general the problems associated with diapycnal transport have caused researchers to avoid this approach.

number of technical issues relating to the intrinsic differences between averages on density surfaces and on level surfaces (i.e., between pseudo-Lagrangian and Eulerian means). The most logical approach to date is the transient-residual-mean (TRM) theory introduced by McDougall (1998, and earlier references therein; hereafter M); McDougall and McIntosh (submitted, hereafter MM) give more detail on the same material. Another, highly related, approach is to use density-weighted averaging (cf. Greatbatch, submitted ms; de Szoeke and Bennett, 1993). The TRM theory applies to low-pass temporally averaged quantities, and deduces a quasi-Stokes velocity $\mathbf{u}^+$ which is related, but not identical, to the bolus velocity. (The two are not identical because the background mean flow involves averages on two different surfaces, though they are frequently similar.) Formulae have been derived for small perturbations by M and MM, involving only averages at constant depth. The quasi-Stokes vector streamfunction is given to second order in amplitude by

$$\Psi = -\frac{\overline{\mathbf{u}_H \rho'}}{\bar{\rho}_z} + \frac{\mathbf{u}_{Hz}}{\bar{\rho}_z}\left(\frac{\bar{\phi}}{\bar{\rho}_z}\right), \qquad (1.3)$$

where the suffix H denotes the horizontal component, and $\phi = (1/2)\rho'^2$. The vertical derivative of Ψ is the horizontal component of $\mathbf{u}^+$.

Two other fundamental differences are (a) that the two-dimensional bolus velocity is intrinsically divergent, while the quasi-Stokes velocity is (by construction) non-divergent, and (b) that the bolus velocity has no diapycnal component while the quasi-Stokes velocity does. Indeed, there is no completely adiabatic expression involving a quasi-Stokes streamfunction.

Since eddying motions are believed to conserve density, this implies that the definition of density must be modified. M shows that rather than using the Eulerian mean density $\bar{\rho}$ at a (vertical) point (EMD for short), one should interpret density as being the inversion of the mean depth of a given density (termed the 'modified mean density' $\tilde{\rho}$ or MMD for short). The difference between these two fields $\tilde{\rho}$ and $\bar{\rho}$ is again of second order in small quantities and is thus very small where the TRM theory is formally valid. However, the time derivatives of EMD and MMD differ by O(1) amounts because of the above discussion. The MMD is advected by the (Eulerian) mean flow and by the quasi-Stokes velocity:

$$\tilde{\rho}_t + \nabla \cdot [(\bar{\mathbf{u}} + \mathbf{u}^+)\tilde{\rho}] = 0. \qquad (1.4)$$

We shall see that near horizontal boundaries, the small-amplitude formulae of M and MM to convert EMD to MMD break down. In fact, the two fields differ at first, not second, order in the small quantities. (This is nothing to do with the question of neutrally stable and mixed layers, which are beyond the scope of this paper.)

Indeed, other questions about horizontal boundaries exist even for finite amplitude motions, and this paper will be mainly devoted to such questions, especially as they relate to eddy parameterisations. For example, the quasi-Stokes streamfunction requires boundary conditions at rigid surfaces. The horizontal component of $\mathbf{u}^+$ is related to the horizontal components of $\mathbf{u}'$ and $\mathbf{u}$, and so vanishes on vertical sidewalls. The value of w^+, the vertical component of $\mathbf{u}^+$, at surface or floor is less obvious. (Unlike the horizontal component of the quasi-Stokes velocity, there is no *kinematic* reason for w^+ to vanish, since w^+ exists to satisfy continuity.)

The problems are best seen by considering recent direct eddy-resolving computations [that by Rix and Willebrand (1996) did not discuss the shape of either bolus or quasi-Stokes velocity] and an eddy-permitting calculation (FRAM, analyzed by McIntosh and McDougall, 1996).

The three eddy-resolving calculations used a re-entrant channel geometry; all used long time and space averages, and so differ subtly – but probably not in any important manner – from the low-pass time average of the TRM theory (indeed, M does not define the averaging process in any way). Values of the equivalent total streamfunction ψ were diagnosed from this average and presented on z-co-ordinates by superimposing them on the EMD.

An immediate problem ensues, generic to this type of activity, caused by the different choices for 'mean' density, and indicated schematically in Fig. 1 (Treguier, Held and Larichev, 1997 give some discussion on this but mainly from the perspective of diabatic surface effects). Suppose that the surface (or bottom) density varies over the averaging period as shown in Fig. 1a. The time-mean is $\bar{\rho}(0)$. The densities lighter than $\bar{\rho}(0)$ are shown shaded. In Fig. 1b, the streamfunction ψ for the total (mean plus eddy) flow is shown as a function of density. If 'density' is taken to be the EMD, then the fluxes associated with the shaded fluid are ignored, producing an apparently non-

zero streamfunction at the surface?[2] There is, simply, nowhere to 'put' the extra fluxes in an Eulerian sense.

The streamfunction is clearly zero at the minimum density: no fluid ever enters at lighter densities. Equally true is that the streamfunction is nonzero at the density $\bar{\rho}(0)$. The question, which is far from just philosophical, is how to interpret mean 'density' in a non-eddy-permitting model.

Some readers may be surprized at this statement. After all, M has argued cogently for the definition to be MMD. This causes both the total and quasi-Stokes streamfunctions to vanish at the surface and floor. For realistic finite amplitude fluctuations, however, the streamfunction changes rapidly very close to the surface, as we shall show. Most non-eddy-resolving models are unlikely to resolve the scale over which this changes, so that they would fail to reproduce the lightest density layers, and act as if the streamfunction had something approximating to a delta-function near-surface. If this layer is not resolved, the quasi-Stokes streamfunction cannot vanish at what is now the surface, inducing an apparent flux through the surface to represent the 'missing' flux on lighter density surfaces. In other words, there may well be a difference – which will be addressed in this paper – between the correct description, using MMD, and the description in an under-resolved model or one using an eddy parameterisation, which may for numerical or physical reasons be using a density field truncated near surface and floor and so resembling the EMD.

In confirmation of this discussion, Killworth (1998) found it impossible to produce a streamfunction which vanished at top and bottom. Indeed, the streamfunction attained *extreme* values at the surface and floor. If other simple numerical inaccuracies were disguising a true zero value at surface and floor, or there were a damping down near surface and floor as suggested by M, one would expect a reduction in its value from the interior as the horizontal boundaries are approached; this is not seen.

Treguier (1999) used an extensive eddy-resolving channel computation to diagnose both v^* and w^* eddy-induced velocities on density surfaces, as well as the quasi-geostrophic version of v^+ and w^+. The two sets of velocities were found to be very similar except near the surface, indirectly

---

2 This problem is not, of course, unique to oceanography; Held and Schneider (1999) have discussed a possible atmospheric solution.

confirming M. However, Treguier's Fig. 7b shows clearly that w^* reaches extreme values at the surface and floor, rather than vanishing. Gille and Davis (1999) ran channel models, both of the

Eddy problem and of a wind-forced problem, and diagnosed the eddy terms. In their Fig. 7, they show what is the majority of the TRM streamfunction, which again does vanish at the surface (it is small at depth, so that no conclusions can be drawn from their figure as to whether the streamfunction vanishes at the floor). McIntosh and McDougall (1996) plotted overturning streamfunction, computed from FRAM, on MMD (their Fig. 4) and on EMD (their Fig. 5). It is clear that the latter case – albeit computed with M's interior formulae and so in error near-surface – does not capture the additional near-surface and floor fluxes which their Fig. 4 does.

These direct calculations, then, indicate that the boundary conditions applied to quasi-Stokes vertical velocities in parameterisations, which historically are consistently those of zero flow at rigid surfaces, need investigation. Particularly, what differences are produced in simulations if the requirement of vanishing w^+ at surface and floor are relaxed? To reiterate, if the physics of the model being employed – e.g. some eddy parameterisation – fails to reproduce the fine density structure, it is not clear we would wish w^+ to vanish.

Following a discussion of the small amplitude theory used by M and MM, the behaviour of the MMD near horizontal boundaries is discussed (section 2). We show that the differences between EMD and MMD become *first* order in small quantities in such regions, suggesting that formulae such as M's, based on small-amplitude theory, will first become invalid for finite amplitude near horizontal boundaries. For finite amplitude, the depth range over which these larger differences occurs is a vertical isopycnal excursion in a deformation radius, and remains too small for current climate models to resolve. Thus EMD and MMD look similar within climate models. The mass of a vertical column is the same using either definition of density, but the potential energy of the column differs: the EMD is the low-pass filtered time mean of the potential energy, while the MMD is consistently smaller. We then show that products of perturbations (e.g. fluxes) exhibit a decay to zero near the boundary using MMD, with the quasi-Stokes horizontal velocity exhibiting a delta-function behaviour.

Small-amplitude theory (section 3) is used to evaluate the relevant expressions making up either the flux divergence or the vector streamfunction. Small-amplitude theory has its disadvantages, but it is at least an exact solution to the equations of motion in the limit of vanishingly small perturbations; it is also accurate to precisely the same order as the M and MM theory. We show specifically that w^+ and the quasi-Stokes streamfunction do not vanish at surface or floor using the M formulae. En route, two equivalents of the isopycnal co-ordinate parameterisation of Killworth (1997), which had been restated as a z-co-ordinate version in that paper without proof, are produced (section 4). Section 5 then briefly discusses these results, comparing them with the Killworth (1997), showing how the delta-functions at surface and floor present in that theory become precisely the vertical quasi-Stokes velocity computed at surface and floor from the second-order M formulae. Section 6 evaluates closed-form solutions for the Eady (1949) problem. We show (section 7) more generally that mass and energy conservation holds for the EMD formulation, but energy conservation does not hold for the MMD formulation even if exact expressions are used through the entire water column, for reasons described earlier.

Section 8 asks the question: given that current climate models cannot resolve the differences between densities, can current eddy parameterisations? We revisit a test of parameterisations (Killworth, 1998), run both with and without the vertical quasi-Stokes velocity vanishing at the surface and floor in two parameterisation schemes. We find that the non-zero surface vertical quasi-Stokes velocity results are uniformly poor compared with zero values. However, an alternative parameterisation, using a direct estimate of the density flux divergence in z-co-ordinates, performs just as well, and would be relevant for an Eulerian definition of mean density. We conclude that parameterisations using quasi-Stokes formulations – which should formally reproduce the MMD – do apparently perform better with no advection through surface and floor, but reproduce the EMD.

2. Eulerian and modified mean densities near a horizontal boundary

(a) Small amplitude

Both M and MM have derived formulae connecting Eulerian and isopycnic averages for the case when perturbations are of small amplitude. In particular, the MMD and EMD are connected by

the relationship

$$\tilde{\rho} = \bar{\rho} + \hat{\rho}$$ (2.1)

where

$$\hat{\rho} = -\left(\frac{\phi}{\bar{\rho}_z}\right)_z$$ (2.2)

and ϕ is half the density variance:

$$\phi = \frac{1}{2}\overline{(\rho'^2)}.$$ (2.3)

Thus if α is a representative amplitude of the small perturbations,

$$\tilde{\rho} = \bar{\rho} + O(\alpha^2)$$ (2.4)

although (examples will be given later) the rate of change of the two densities, being $O(\alpha^2)$, can be quite different.

The relationship (2.1) has been tested by various authors using output from numerical models and (2.4) holds quite well. Both the relationship (2.1) *and* the deduction (2.4) break down near a horizontal surface. That they must break down is of course clear for finite amplitude excursions, and M suggests modifications to turbulent diffusions [but not to (2.1) or (2.4)] accordingly. However, the relationship *also* breaks down at small amplitude (i.e., for which the formulae are formally accurate), but with a much larger error than in the interior. The manner of this breakdown is as follows.

Suppose that near some horizontal surface $z = z_0$, the relationship between density and depth is given by

$$z - z_0 = F(\rho - \rho_0) + \alpha G(\rho - \rho_0, t)$$ (2.5)

where ρ_0 is some measure of the density 'near' the surface, F is some function of density whose gradient is negative for stably stratified fluid, and G, of amplitude order unity, represents the time variation of the depth surface.[3] We assume $F'(0) = 0$ without loss of generality. The use of density co-ordinates means that MMD can be calculated exactly. Define a low-pass average of some quantity K on a density surface as

---

[3] This variation is produced by unspecified three-dimensional motions; the dependence on horizontal position is irrelevant for the current discussion.

$$\bar{K} = \frac{1}{T} \int_0^T K \, dt$$

and since G is a perturbation,

$$\bar{G} = 0.$$

Then, providing z is 'some way below' z_0, (assuming this is the upper surface) a time average gives

$$\overline{z - z_0} = \overline{F(\rho - \rho_0)}$$

or, inverting,

$$\tilde{\rho} - \rho_0 = F^{-1}(z - z_0)$$

where we have used the definition of MMD in the inversion. Since we have from M that $\tilde{\rho} - \bar{\rho} = O(\alpha^2)$, to *first* order $\tilde{\rho}$ and $\bar{\rho}$ are identical.

Now suppose z is within $O(\alpha)$ of z_0. We write

$$z - z_0 = \alpha\xi, \quad \rho - \rho_0 = \alpha r$$

and substitute into (2.5):

$$\alpha\xi = F(\alpha r) + \alpha G_0(t) + \alpha G(\alpha r, t)$$

$$= \alpha r F_\rho + \frac{1}{2}\alpha^2 r^2 F_{\rho\rho} + ... + \alpha G_0(t) + \frac{1}{2}\alpha^2 G_1(t) + ... \qquad (2.6)$$

where a suffix denotes derivatives, F derivatives are evaluated at $\rho = \rho_0$ and $G_0 = G(0, t)$, $G_1 = G_\rho(0, t)$, etc. To leading order this gives

$$\xi = r F_\rho + G_0(t). \qquad (2.7)$$

Suppose now that G_0 varies between G_{min} and G_{max} for some $G_{min} < 0$, $G_{max} > 0$ of order unity. Then when ρ (or equivalently r) becomes sufficiently light, ξ becomes negative and a region above the fluid surface is predicted from (2.7). Thus the averaging over time must be taken only when $\xi \le 0$. But there will be an average ξ for any density which ever occurs in the fluid column; and the range of density variation is $O(\alpha)$.[4]

This immediately means that the least density which ever occurs [which will be $\tilde{\rho}(z_0)$] is $O(\alpha)$ less than ρ_0 [which will in turn be shown to be $\tilde{\rho}(z_0)$ to leading order], so that near surface and floor

---
[4] There is apparently a choice whether to compute the average value of ξ only during the time that density is present, or to compute the full average, defining z to be at the surface or floor at other times. Surprisingly, the former choice yields multivalued ξ, i.e. two mean densities with the same depth.

EMD and MMD differ by $O(\alpha)$, much larger than the $O(\alpha^2)$ they differ by in the interior. Thus the locations where the M and MM formulae first break down are near surface and floor, and in such places the errors are likely to be much higher than the third order predicted by theory.

To proceed, we have

$$\bar{\xi} = \frac{1}{T} \int_{\xi < 0} [r F_\rho + G_0(t)] \, dt \qquad (2.8)$$

where the range of densities where the integration is restricted is

$$-\frac{G_{min}}{F_\rho} \le r \le -\frac{G_{max}}{F_\rho}.$$

Defining

$$A(x) = \frac{1}{T}\int_{G_0(t) \le x} dt; \quad B(x) = \frac{1}{T}\int_{G_0(t) \le x} G_0(t)\, dt \qquad (2.9)$$

we have immediately

$$A(G_{min}) = 0; \quad A(G_{max}) = 1$$
$$B(G_{min}) = 0; \quad B(G_{max}) = 0$$

and so

$$\bar{\xi} = r F_\rho A(-r F_\rho) + B(-r F_\rho). \qquad (2.10)$$

Straightforward evaluation shows the following:

$$\bar{\xi} = 0,\ \bar{\xi}_\rho = 0, \quad \text{when } r = -\frac{G_{min}}{F_\rho} \text{ (the lightest fluid ever present)}$$

$$\bar{\xi} = r F_\rho, \quad \text{when } r = -\frac{G_{max}}{F_\rho} \text{ (the lightest fluid which never outcrops at the surface).} \qquad (2.11)$$

Thus the lightest fluid has a zero-thickness layer at the surface, and the densest fluid to ever outcrop at the surface blends smoothly into the interior solution.

The EMD is computed by setting $z = z_0$ in (2.5), and expanding for small perturbations,

$$F(\rho - \rho_0) + \alpha G(\rho - \rho_0, t) = 0, \text{ i.e.,}$$

$$\alpha r F_\rho + ... + \alpha G_0(t) + ... = 0 \text{ to leading order}$$

giving $r(z_0) = 0$. Thus

$$rF_\rho = -G_0(t)$$

As stated, the two densities differ at *first*, not *second*, order in small quantities.

$$\bar\rho(z = z_0) = \rho_0 + O(\alpha^2)$$

$$\tilde\rho(z = z_0) = \rho_0 - \alpha\frac{G_{min}}{F_\rho}.$$

This is indicated schematically in Fig. 2, which also shows a specific example, for which $F_\rho = -1$ and $G_0(t) = \sin(t)$. To reiterate, $\bar\rho$ and $\tilde\rho$ are very similar in the interior (for small amplitude) but differ much more strongly near surface and floor, in a manner similar to a delta-function.

(b) *Finite amplitude*

At finite amplitude the difference between EMD and MMD become more important. Note that the depth over which this difference is large is proportional to the amplitude of the perturbations. Finite amplitude density fluctuations will equilibrate at about $a\nabla_H\bar\rho$, where a is the deformation radius and ∇_H the horizontal gradient operator. This implies that the vertical scale is

$$z' \sim \rho'/\bar\rho_z \sim a|\nabla_H\bar\rho/\bar\rho_z|$$ (2.12)

as suggested by M. It is the typical vertical excursion made when moving a short horizontal distance (a) along a mean isopycnal which moves significantly vertically only on the gyre scale ($L \gg a$).

This scale is rather small for the ocean, though not for the atmosphere. Even with fairly optimistic estimates, it is hard to produce a vertical scale much larger than 20 m. So *the distance over which the MMD and EMD differ significantly is not resolved in most climate models*, being concentrated in the last grid point. Thus the near-boundary differences between the two mean densities will probably appear to climate models as single grid-point effects, i.e. delta functions.

Figure 3 shows this effect clearly (also cf. McIntosh and McDougall, 1996, for example). It shows a four-year along-channel average of Eulerian mean and modified mean temperatures for an

eddy-permitting channel run. (A similar diagram for the previous four years is visually indistinguishable from this.) The north and south boundaries are relaxed to specified linear temperature gradients, and the surface heat flux is a relaxation to a linear function of latitude. The grid spacing was 10 km horizontally, and 10 m vertically. The high lateral gradients and forcing were designed to increase the depth over which the EMD and MMD differ significantly to a value which the model could resolve. In this case, an estimate of the horizontal length scale of variability is NH/f where N is the buoyancy frequency. With the values here, (2.12) yields a depth of 50–60 m. Fig. 3 confirms this approximately; the main differences are confined to the upper 100 m. The 'pushing forward' of the isotherms from further south at the surface is very clear. Differences are very small at the lower boundary because eddy amplitudes were small there also.

The presence of a mixed layer (not treated here) makes no difference to this argument, since it merely moves the region where EMD and MMD differ slightly lower (usually to worse resolution).

Also shown in Fig. 3 is a typical two-dimensional parameterisation result, in this case using the Gent and McWilliams (1990) formulation, though as we shall see later, all extant parameterisations are similar in behaviour. While it is clear that the parameterisation fails to do a good job in the upper southern portion, it is also obvious that there is no hint of the 'pushing forward' of surface isotherms present, despite – deliberately – there being ample vertical resolution. Thus under most circumstances extant parameterisations cannot resolve the differences between EMD and MMD, and when they can, they do not reproduce the MMD structure. This will be discussed in more detail below.

(c) *Mass and potential energy*

The differences between the two densities have two important effects. The first is directly concerned with the interpretation of mean density. It is straightforward to see that the low-pass time filtered net mass in a water column, which is a uniquely defined value, is the same whether EMD or MMD is used:

$$\overline{\int \rho\,dz} = \int \bar\rho\,dz \text{ (averaging at constant depth)}$$

= ∫ ρ z_ρ dρ = ∫ ρ̄ z_ρ dρ = ∫ ρ̄ z dz (averaging at constant density).

(As Fig. 2 suggests, $\tilde{\rho}$ is lighter at the surface, but the shortfall is made up at the floor.)

The same does *not* hold for potential energy, because of the noncommutative averaging operators on products of quantities. For small amplitude, the differences between EMD and MMD potential energies are O(α^3), and occur due to O(α^2) differences in the interior over a depth range of order unity, and O(α) differences over O(α^2) depth ranges. Formally, we write

$$\Delta\rho \equiv \tilde{\rho} - \bar{\rho} = -\alpha^2 \lambda_z + \alpha a(z) \qquad (2.13)$$

where $\alpha^2 \lambda$ is $(\phi/\bar{\rho}_z)$ and the second term is the surface decrement and floor increase in density. From its definition, $\lambda < 0$. Eqn. (2.13) does not include the smaller, O(α^2), corrections to the formulae near surface and floor since these will be unimportant to the depth integrals. Since the total mass of the column is invariant,

$$\int_{-H}^{0} \Delta\rho \, dz = 0 \Rightarrow \alpha [\lambda]_{-H}^{0} = \int_{-H}^{0} a(z) \, dz \equiv \int_{floor} a(z) \, dz + \int_{surface} a(z) \, dz \qquad (2.14)$$

where we split the a integral into two sub-integrals at floor and surface. The first is positive (the MMD is denser than EMD), the second negative.

The difference in potential energy, invariant to changes in vertical co-ordinate origin, is

$$\Delta PE = \int_{-H}^{0} z (\tilde{\rho} - \bar{\rho}) \, dz = \int_{-H}^{0} z \Delta\rho \, dz$$
$$= \int_{-H}^{0} z[-\alpha^2 \lambda_z + \alpha a(z)] \, dz$$
$$= -\alpha^2 [z\lambda]_{-H}^{0} + \alpha^2 \int_{-H}^{0} \lambda \, dz + \alpha \left\{ (0) \int_{surface} a(z) \, dz + (-H) \int_{floor} a(z) \, dz \right\} \qquad (2.15)$$

where we have retained the multiplicand at the surface for clarity, and higher order terms are neglected.

Substituting for the floor integral from (2.14), (2.15) becomes

$$\Delta PE = -\alpha^2 H \lambda_{-H} + \alpha^2 \int_{-H}^{0} \lambda \, dz - \alpha H \left\{ \alpha (\lambda_0 - \lambda_{-H}) - \int_{surface} a(z) \, dz \right\} - \int_{surface} a(z) \, dz$$
$$= -\alpha^2 H \lambda_0 + \alpha^2 \int_{-H}^{0} \lambda \, dz + \alpha H \int_{surface} a(z) \, dz - \int_{surface} a(z) \, dz < 0 \qquad (2.16)$$

since all three terms in the sum are negative.

The difference between the two PE expressions lies in the variability, fundamentally a part of the MMD. It involves an integral in density space of the mean square depth fluctuations; the proof is straightforward, either from the M formula or by direct evaluation, and is not given here.

Thus *the low-pass filtered potential energy of a fluid column (a uniquely defined quantity) is only correctly evaluated using EMD, and is consistently underestimated using the MMD;* correction terms can be derived, and involve knowledge of the variability.

3. Local instability theory in z-co-ordinates

In this section, we extend linear instability theory beyond the quasigeostrophic limit, using vertical co-ordinates, using a local approach similar to that of Robinson and McWilliams (1974). Linear theory is not always a good predictor of the behaviour of a nonlinear eddying system, as Edmon et al. (1980) show clearly for the quasi-geostrophic limit. (Note that the TRM formulae of M and linear instability theory are both small amplitude, both evaluated to second order, and hold in the same parameter ranges.) We begin by assuming that

$$\varepsilon = \frac{a}{L} \qquad (3.1)$$

is a small quantity, where

$$a = \frac{(g'H)^{1/2}}{f_0}$$

remains the local deformation radius, and L the horizontal length scale, $g' = g\Delta\rho/\rho_0$ is a reduced gravity based on a typical top-to-bottom density change $\Delta\rho$ and H is a typical depth. The horizontal variation of density may be less than or equal to the vertical variation. In subpolar gyres, where isopycnals outcrop at surface and floor, equality would be relevant. In quasigeostrophic circumstances, the horizontal variation $\Delta\rho_H$ would be much less than the vertical. We thus pose a horizontal variation $\Delta\rho_H \sim \sigma\Delta\rho$ for what follows, where σ is either smaller, or much smaller, than 1. We finally assume (following quasigeostrophic theory, but not bound by it) that f, the Coriolis parameter, changes little over a scale a, so that

$$\frac{\beta a}{f_0} \approx \sigma\epsilon. \tag{3.2}$$

Here the additional factor σ ensures that stretching of planetary vorticity does not dominate the vorticity balance [(3.2) is equivalent to $\beta a^2/u \approx 1$.]

From thermal wind, $\bar{\mathbf{u}}$, and hence the phase speed c defined below, scale with $\sigma g'H/f_0 L = \epsilon\sigma a f_0$. Then a basic background structure which is geostrophic, hydrostatic, etc. gives the remaining scalings for the mean flow as

$$\frac{\bar{p}}{\rho_0} \approx g'H; \quad \bar{w} \approx \frac{\beta H}{f_0}\bar{u} \text{ (from vortex stretching)} \approx \epsilon^2\sigma^2 Hf_0.$$

What this will mean is that $\bar{w}$ terms will be as important as the horizontal u', v' terms.

We seek a small perturbation to background flows proportional to $\exp ik(x\cos\theta + y\sin\theta - ct)$, where k will be O(a^{-1}). If the problem has a channel geometry, then θ is zero in what follows. Scalings for the perturbation terms, and quantities derived therefrom, are given in Appendix A. The horizontal momentum equations become

$$ik(\bar{u} - c)u - fv = -i\frac{k\cos\theta}{\rho_0}p + \text{small}$$

$$ik(\bar{u} - c)v + fu = -i\frac{k\sin\theta}{\rho_0}p + \text{small}$$

where "small" includes terms in, e.g., $u\bar{u}_x$, etc., which are O(ϵ) smaller than the terms retained. The density equation becomes, similarly,

$$ik(\bar{u} - c)\rho + u\bar{\rho}_x + v\bar{\rho}_y + w\bar{\rho}_z = 0 + \text{small}$$

where $\tilde{u} \equiv \bar{u}\cos\theta + \bar{v}\sin\theta$ is usefully defined, and "small" again includes terms in $\rho\nabla\bar{u}$, etc.[5]

Finally mass conservation and the hydrostatic relation give

$$u_x + v_y + w_z = 0$$

$$p_z = -g\rho.$$

[5] The confirmation that the neglected terms remain small even after the vorticity equation is created is tedious and not shown here.

Cross-differentiating the momentum equations (the neglected terms remain small)) and use of mass conservation, gives

Now density conservation implies

$$fw_z = -i\frac{k^3(\bar{u} - c)}{\rho_0 f}p + i\frac{k\cos\theta}{\rho_0 f}\beta p.$$

so that elimination of w' gives the familiar quasi-geostrophic equation

$$(\bar{u} - c)\left\{\left(\frac{f^2 p_z}{N^2}\right)_z - k^2 p\right\} + \bar{q}_y p = 0 \tag{3.4}$$

with boundary conditions of zero w' at top and bottom. Here

$$\bar{q}_y = \beta\cos\theta - \left(\frac{f^2}{N^2}\tilde{u}_z\right)_z$$

is the mean quasi-geostrophic potential vorticity gradient normal to the direction θ; the subscript y has been retained for historical purposes (in a channel geometry this would be precise). It is also $\bar{\rho}_z$ times the along-isopycnal gradient of the mean Ertel potential vorticity. To see this, note that with planetary scalings, this vorticity is merely $f\bar{\rho}_z$. The gradient of this in (say) the y-direction, holding density constant, is

$$[\partial/\partial y - (\rho_z/\bar{\rho}_z)\partial/\partial z](f\bar{\rho}_z) = \bar{\rho}_z[\beta + f(\bar{\rho}_z/\bar{\rho}_z)] = \bar{\rho}_z[\beta - (f^2\bar{u}_z/N^2)_z],$$

with a similar expression in the x-direction. Combining these gives $\bar{q}_y$ as the gradient of the potential vorticity normal to θ.

We first find expressions for the quantities necessary for $\nabla \cdot (\mathbf{u}\overline{\rho'})$ from small-amplitude theory. We have, by standard methods (e.g., Killworth, 1997):

$$\overline{u'\rho'} = \frac{1}{2}\text{Re}\left(-i\frac{k\sin\theta}{f\rho_0}p \cdot \frac{p_z^*}{g}\right) = \frac{k\sin\theta}{2f\rho_0 g}\text{Re}(ipp_z^*) \tag{3.5}$$

$$\overline{v'\rho'} = \frac{1}{2}\text{Re}\left(i\frac{k\cos\theta}{f\rho_0}p \cdot \frac{p_z^*}{g}\right) = \frac{k\cos\theta}{2f\rho_0 g}\text{Re}(ipp_z^*)$$

$$\overline{w'\rho'} = \frac{1}{2}\text{Re}\left\{\frac{ik}{\rho_0 N^2}[(\bar{u} - c)p_z - \bar{u}_z p] \cdot \frac{p_z^*}{g}\right\} \tag{3.6}$$

$$= \frac{kc_i}{2g\rho_0 N^2}|p_z|^2 - \frac{k\bar{u}_z}{2g\rho_0 N^2}\text{Re}(ipp_z^*).$$ (3.7)

Here an asterisk means a complex conjugate. The averages are over either one real period of the growing mode or, equivalently, over one horizontal cycle of the instability. The scalings in Appendix A show that the dominant terms acting to change the mean density are the horizontal advection terms $\nabla_H \cdot (\overline{\mathbf{u}_H \rho})$, though it will appear that the vertical term, formally $O(\sigma)$ less, and neglected in quasigeostrophic theory, acts to change the potential energy.

We can also compute expressions from the small-amplitude TRM theory which hold away from horizontal boundaries. First, we have

so that

$$\bar\phi = \frac{1}{2}\overline{(\rho'^2)} = \frac{1}{4g^2}|p_z|^2$$

$$\hat\rho = \frac{1}{4\rho_0 g}\left(\frac{|p_z|^2}{N^2}\right)_z.$$ (3.8)

For the x-component, we need

$$\psi_1 = -\frac{\overline{u'\rho'}}{\bar\rho_z} + \frac{\bar u_z}{\bar\rho_z}\left(\frac{\bar\phi}{\bar\rho_z}\right)$$

and for the y-component

$$\psi_2 = -\frac{\overline{v'\rho'}}{\bar\rho_z} + \frac{\bar v_z}{\bar\rho_z}\left(\frac{\bar\phi}{\bar\rho_z}\right).$$

Appendix A shows that the second terms are O ($\varepsilon\sigma$) smaller than the first, and so can be neglected under the assumptions here. However, in regions of weak vertical stability, e.g. the subpolar regime, this may not be the case. For completeness, we retain both terms in what follows, but maintain the order of appearance of the terms for clarity. Then, from above,

$$\psi_1 = \frac{k\sin\theta}{2f\rho_0^2 N^2}\text{Re}(ipp_z^*) + \frac{\bar u_z}{4\rho_0^2 N^4}|p_z|^2$$ (3.9)

and

$$\psi_2 = \frac{k\cos\theta}{2f\rho_0^2 N^2}\text{Re}(ipp_z^*) + \frac{\bar v_z}{4\rho_0^2 N^4}|p_z|^2.$$ (3.10)

For use in parameterisation schemes, we can calculate the following expression involving $\text{Re}(ipp_z^*)$.

We begin from a restatement of the quasi-geostrophic equation,

$$\left(\frac{p_z}{N^2}\right)_z = \frac{f^2}{\bar u - c}\{k^2(\bar u - c) - q_y\}.$$

We then note that

$$\frac{\partial}{\partial z}\text{Re}\left(\frac{ipp_z^*}{N^2}\right) = \text{Re}\left(ip\left[\frac{p_z^*}{N^2}\right]_z\right) = -\frac{c_i\bar q_y}{f^2}\frac{|p|^2}{|\bar u - c|^2}$$

after a little algebra. If we introduce the diffusivity

$$\kappa = \frac{kc_i}{2f^2\rho_0^2}\left.\frac{|p|^2}{|\bar u - c|^2}\right|,$$ (3.11)

then

$$\frac{\partial}{\partial z}\text{Re}\left(\frac{ipp_z^*}{N^2}\right) = -2\kappa\bar q_y\rho_0^2/k.$$

Using the boundary condition at, say, $z = 0$, which yields

$$(\bar u - c)p_z = \bar u_z p, \quad z = 0, -H$$

we can integrate the above to yield

$$\text{Re}\left(\frac{ipp_z^*}{N^2}\right) = \left.\frac{\bar u_z|p|^2 c_i}{N^2|\bar u - c|^2}\right|_{z=0} - \frac{c_i}{f^2}\int_0^{\bar z}\frac{|p|^2\bar q_y}{|\bar u - c|^2}dz.$$ (3.12)

Then, returning to the quasi-Stokes velocities,

$$u^+ = \psi_{1z}, \quad v^+ = \psi_{2z}$$

giving

$$u^+ = \frac{k\sin\theta}{2f\rho_0^2}\frac{\partial}{\partial z}\text{Re}\left(\frac{ipp_z^*}{N^2}\right) + \frac{1}{4\rho_0^2}\frac{\partial}{\partial z}\left(\bar u_z\frac{|p_z|^2}{N^4}\right)$$

$$= -\frac{k\sin\theta}{2f\rho_0^2}\frac{c_i\bar q_y|p|^2}{f^2|\bar u - c|^2} + \frac{1}{4\rho_0^2}\frac{\partial}{\partial z}\left(\bar u_z\frac{|p_z|^2}{N^4}\right)$$

$$= -\frac{\kappa\sin\theta}{f}\bar q_y + \frac{1}{4\rho_0^2}\frac{\partial}{\partial z}\left(\bar u_z\frac{|p_z|^2}{N^4}\right)$$ (3.13)

and

$$v^+ = -\frac{\kappa\cos\theta}{f}\bar q_y + \frac{1}{4\rho_0^2}\frac{\partial}{\partial z}\left(\bar v_z\frac{|p_z|^2}{N^4}\right).$$ (3.14)

Recall that the second terms in in (3.13), (3.14) are usually small compared with the first terms, so that the quasi-Stokes velocities are simply proportional to the diffusivity (which is a function of position) times the potential vorticity gradient. As shown by Killworth (1997), linear theory implies that potential vorticity is mixed (together with a possible rotation term), and not thickness.

The scalings in Appendix A show that the main term acting to change the mean density is now the pseudo-vertical term $w^+\bar{\rho}_z$, with the horizontal terms smaller by O(σ). Thus the horizontal terms dominate in the divergence formulation, but the *vertical* term is important in the quasi-Stokes formulation, as discussed in detail by Treguier et al. (1997).

It is enlightening to connect these two formulations formally. Let us denote the two terms in the expression (3.7) for $\overline{w'\rho}$ respectively as A and B. Then, noting that a time derivative of a quadratic quantity involves multiplication by $2kc_i$, we have immediately

$$\hat{\rho}_t = A_z.$$

(3.15)

Similarly,

$$B = -\frac{k}{2g\rho_0 N^2}(\bar{u}_z \cos\theta + \bar{v}_z \sin\theta)\,\text{Re}(ipp_z^*)$$

$$= \frac{f}{N^2}\left(\bar{u}_z\overline{v'\rho'} - \bar{v}_z\overline{u'\rho'}\right)$$

$$= \frac{g}{\rho_0 N^2}\overline{\mathbf{u}_H^+\rho'}\cdot\nabla_H\bar{\rho}$$

$$= \left(\Psi - \frac{\mathbf{u}_{Hz}}{4\rho_0^2 N^2}|p_z|^2\right)\cdot\nabla_H\bar{\rho}$$

$$= \Psi\cdot\nabla_H\bar{\rho}$$

since the second term vanishes by thermal wind balance. Thus

$$(\overline{w'\rho'})_z = A_z + B_z$$

(3.16)

Similarly, we can compute from (3.9), (3.10),

$$\nabla_H\cdot(\overline{\mathbf{u}_H'\rho'}) = -\nabla_H\cdot(\Psi\bar{\rho}_z) + \nabla_H\cdot\left(\mathbf{u}_H\frac{\bar{\phi}}{\bar{\rho}_z}\right)$$

where the scalings in Appendix A show that the second term is O(ϵ) smaller than the first and so is neglected. Adding, we find

$$\nabla\cdot(\overline{\mathbf{u}'\rho'}) = \hat{\rho}_t + \mathbf{u}_H^+\cdot\nabla_H\bar{\rho} - \bar{\rho}_z\nabla_H\cdot\Psi = \hat{\rho}_t + \mathbf{u}^+\cdot\nabla\bar{\rho}$$

(3.17)

demonstrating for linear theory that the two approaches are identical.

At the surface (or floor) we can evaluate ψ_1 and ψ_2, and hence w^+, using the interior formulations, which as we have seen will be seriously in error near the boundary. Indeed,

$$\psi_1 = \frac{k\sin\theta}{2f\rho_0^2 N^2}\text{Re}\left(i\frac{p\bar{u}_z}{|\bar{u}-c|^2}(\bar{u}-c)p^*\right) + \frac{\bar{u}_z}{4\rho_0^2 N^4}|p_z|^2, \quad z = 0, -H$$

$$= \frac{|p|^2}{2\rho_0^2 N^2|\bar{u}-c|^2}\left\{\frac{kc_i\bar{u}_z\sin\theta}{f} + \frac{\bar{u}_z^2}{2N^2}\right\}, \quad z = 0, -H$$

$$= \kappa\left(\frac{\bar{u}_z\sin\theta}{N^2} + \frac{f\bar{u}_z^2}{2N^4kc_i}\right), \quad z = 0, -H$$

(3.18)

and

$$\psi_2 = \frac{|p|^2}{2\rho_0^2 N^2|\bar{u}-c|^2}\left\{\frac{kc_i\bar{u}_z\cos\theta}{f} + \frac{\bar{v}_z^2}{2N^2}\right\}, \quad z = 0, -H$$

$$= \kappa\left(\frac{\bar{u}_z\cos\theta}{N^2} + \frac{\bar{v}_z^2}{2N^4kc_i}\right), \quad z = 0, -H.$$

(3.19)

These expressions cannot be zero (else the solution for p would be identically zero at all depths), so that the quasi-Stokes streamfunction, using the M formulation for the interior of the fluid, does not vanish at surface or floor for linear theory. (The correct value goes to zero at surface and floor in a delta-function-like manner.)

For a channel problem, ψ_1 vanishes identically, and the surface and floor values of ψ_2 reduce to

$$\kappa\bar{\rho}_y/\bar{\rho}_z = -\kappa\cdot(\text{slope of isopycnals}),$$

which is precisely of the form suggested by Gent and McWilliams (1990), although it would be set to zero at such locations in their parameterisation.

4. Depth-co-ordinate eddy parameterisations

Linear theory using density co-ordinates was used by Killworth (1997) to create an eddy parameterisation which performed well in a channel model simulation (Killworth, 1998). However, that theory was converted from (e.g.) a formulation for bolus velocity into one for the quasi-Stokes

velocity, without regard for the differences in averaging involved between depth and density co-ordinates. This was done from the perspective that although the two approaches are different, using one approach to suggest an eddy parameterisation in the other remained useful. However, the depth co-ordinate approach was not formally justified by Killworth (1997), although Treguier (1999) shows that simple conversions do in practice work rather well. The formulae of the previous section can be used to produce two linked parameterisation schemes based entirely on depth co-ordinates.

Both approaches start by obtaining approximate solutions to the problem (3.4), yielding good guesses at the wavenumber k, orientation θ, the shape of the eigenvector in the vertical, and finally its amplitude. These are given exactly as in sections 6 and 7 of Killworth (1997). Wavenumber is estimated as $0.5lf/C$, where C is approximately

$$\frac{1}{\pi}\int_{-H}^{0} N(z)\,dz,$$

(C is also used to estimate the deformation radius $a = C/f$), and orientation (not used in the channel problems to follow, where the orientation is identically zero) is given by an approximate maximisation of growth rate. The shape of the eigenvector is given by either of two approximations; in this paper we use two cycles of the iterative procedure in Killworth (1997: section 7), converted directly to depth co-ordinates.

This iteration starts from an approximate form for c:

$$c_0 = \bar{\bar{u}} - \frac{\beta}{2k^2} + i\sqrt{\left(\bar{u}_s^2 - \frac{\beta^2}{4k^4}\right)}$$

(for nonzero orientation the formula is more complicated), where

$$\bar{\bar{u}} = \frac{1}{H}\int_{-H}^{0}\bar{u}\,dz; \quad \bar{u}_s = \left[\frac{1}{H}\int_{-H}^{0}\bar{u}^2\,dz - \bar{\bar{u}}^2\right]^{1/2}$$

are the mean and standard deviation of the mean flow respectively. An initial guess for the eigenvector is taken as $p_0 = \bar{u} - c_0$, or, redefining $\chi = p/(\bar{u} - c)$, $\chi_0 = 1$. We express (3.4) in terms of χ and integrate either top-to-bottom or from bottom to some depth, resulting in iterations for c_{n+1} and χ_{n+1} in terms of their previous iterates. c_{n+1} satisfies a simple quadratic

$$c_{n+1}^2\left[\int_{-H}^{0}\chi_n\,dz\right] + c_{n+1}\left[-2\int_{-H}^{0}\bar{u}\chi_n\,dz + \frac{\beta\cos\theta}{k^2}\int_{-H}^{0}\chi_n\,dz\right] +$$

$$\left[\int_{-H}^{0}\bar{u}^2\chi_n\,dz - \frac{\beta\cos\theta}{k^2}\int_{-H}^{0}\bar{u}\chi_n\,dz\right] = 0.$$

The eigenvector χ_{n+1} is given by

$$\chi_{n+1} = 1 + \frac{k^2}{f^2}\int_{-H}^{\bar{z}}\frac{N^2(z')\,dz'}{(\bar{u}(z') - c_{n+1})^2}\int_{-H}^{\bar{z}}\chi_n\left\{(\bar{u}(z'') - c_{n+1})^2 - \frac{\beta\cos\theta}{k^2}(\bar{u}(z'') - c_{n+1})\right\}dz.$$

This also gives a shape for the diffusivity, since this is proportional to $|\chi|^2$, from (3.11). This nondimensionally (and arbitrarily) has a value unity at the bottom. The scaling for diffusivity is then taken to be $A\,\max(a,\Delta)c_i$, where A is of order unity, $\max(a,\Delta)$ is the larger of the deformation radius and the grid spacing[6], and the inclusion of c_i ensures that there is no mixing in baroclinically stable regions. The diffusivity varies both vertically and horizontally.

The first parameterisation simply evaluates $\nabla \cdot (\overline{\mathbf{u}'\rho'})$ directly, using these scalings and formulae (3.5) to (3.7). This is intrinsically a scaling using EMD $\bar{\rho}$. Since the eddy terms can be evaluated to second order accuracy everywhere, questions of boundary conditions do not enter the formulation: $\nabla \cdot (\overline{\mathbf{u}'\rho'})$ can be evaluated everywhere.

The second parameterisation uses the scalings and approximations to compute the quasi-Stokes streamfunction from (3.9) and velocities from (3.13), (3.14), retaining only the first terms in both cases (which M suggests is almost certainly sufficiently accurate). The top and bottom boundary conditions on streamfunction are temporarily left undefined, for reasons discussed below.

5. The connection with isopycnal co-ordinates

Although many features appear similar between depth and isopycnic co-ordinate approaches, interpretations of means, etc. must of necessity differ, so that care must be taken in taking conclusions from one co-ordinate system and applying them to another. A particular case here is the delta-functions present at surface and floor in the lateral fluxes of Killworth (1997). There it was argued that delta-functions in the bolus velocity of magnitude $\kappa\nabla\bar{\rho}/\bar{\rho}_z$ were required to account for the implicit flattening of the isopycnal surfaces where outcrops impinge on top and

6 See Killworth (1997) for rationale. For the runs here, a is used consistently.

bottom. This flattening represented precisely the near-surface and floor changes due to the MMD.

It is useful to examine the role delta-functions near surface and floor possess in level co-ordinates. We show briefly the following: (a), a necessary condition on the diffusivity which does take the same form in vertical as in isopycnal co-ordinates; and (b), that the delta-function amplitudes are precisely those of the vertical quasi-Stokes velocity at the surface (computed using interior approximations), so that the 'missing' fluxes, which belong to to no available EMD, match precisely the values of the quasi-Stokes streamfunction evaluated using the M (interior) formulae.

a. a necessary condition

We note from (3.13), (3.14) that, using interior formulae,

$$\mathbf{u}^+ = \frac{\kappa\bar{q}_y}{f}\begin{pmatrix} -\sin\theta \\ \cos\theta \end{pmatrix} + \frac{1}{4\rho_0^2}\frac{\partial}{\partial z}\left(\frac{\overline{\mathbf{u}_z|\rho_z|^2}}{N^4}\right)$$ (5.1)

so that, integrating both sides,

$$[\Psi]^0_{-H} = f\mathbf{A}\cdot\int_{-H}^0 \kappa\left(\frac{\nabla_H\bar\rho}{\bar\rho_z}\right)dz + \beta\mathbf{A}_2\int_{-H}^0 \kappa\,dz + \frac{1}{4\rho_0^2}\left[\left(\frac{\overline{\mathbf{u}_z|\rho_z|^2}}{N^4}\right)\right]^0_{-H}$$ (5.2)

where

$$\mathbf{A} = \begin{pmatrix} \sin^2\theta & -\sin\theta\cos\theta \\ -\sin\theta\cos\theta & \cos^2\theta \end{pmatrix}$$ (5.3)

is the turning matrix in Killworth (1997) and $\mathbf{A}_2$ its second column. Integrating the first term on the r.h.s., by parts, use of (3.18), (3.19) on the l.h.s. together with thermal wind, and cancellation of the last terms on both sides yields

$$f\mathbf{A}\cdot\left[\kappa\frac{\nabla_H\bar\rho}{\bar\rho_z}\right]^0_{-H} = f\mathbf{A}\cdot\left[\kappa\frac{\nabla_H\bar\rho}{\bar\rho_z}\right]^0_{-H} - f\mathbf{A}\cdot\int_{-H}^0 \kappa_z\frac{\nabla_H\bar\rho}{\bar\rho_z}dz + \beta\mathbf{A}_2\int_{-H}^0\kappa\,dz.$$ (5.4)

The first terms cancel, leaving Killworth's (1997 eqn. 41a), namely

$$\int_{-H}^0 \frac{\kappa_z}{\bar\rho_z}\mathbf{A}\cdot\nabla_H\bar\rho\,dz = \frac{\beta}{f}\int_{-H}^0\kappa\mathbf{A}_2\,dz.$$ (5.5)

Note that this only uses interior values, and neglects the unresolved boundary layers. For parameterisations such as Killworth (1997), in which κ is well-behaved at surface and floor, the additional contributions are negligible. Using the Gent and McWilliams (1990) formulation where

κ is required to drop to zero at surface and floor would involve extra contributions to the balance (5.5). In all cases, though, some form of this condition is the direct consequence of theory which conserves potential vorticity, though the precise structure will depend on the assumptions made. Green (1970), for example, derived a simplified form.

b. Surface and floor delta-functions

We write, more simply, still using the M formulation for small perturbations which holds *away* from boundaries,

$$[\Psi]^0_{-H} = \int_{-H}^0 \mathbf{u}^+dz = f\mathbf{A}\cdot\left[\kappa\frac{\nabla_H\bar\rho}{\bar\rho_z}\right]^0_{-H}.$$ (5.6)

This expression is precisely the jump in delta-functions used by Killworth (1997) in the isopycnal formulation, but is now shown to be the jump in quasi-Stokes fluxes between surface and floor (at least for small-amplitude theory) which reduces to zero if the density range is extended to include the full range of MMD. Thus the values of w^+ at surface and floor *using the interior M theory* are precisely those needed to account for the divergence of the horizontal quasi-Stokes fluxes; they play the same role as the delta-functions in isopycnal theory. The rapid changes near surface and floor only exist in terms of MMD, because they relate to $\mathbf{u}^+$. EMD is modified only by $\nabla\cdot(\overline{\mathbf{u}\rho})$, which possesses no anomalous behaviour anywhere in the fluid.

6. A special case – the Eady problem

We consider, in parallel, two cases. The first considers what is essentially an infinitely wide channel, in which the maximum growth rate is achieved by a wavenumber directed along-channel. In this case the eddy amplitude is the same at all values of y. The second retains structure cross-channel, as in the original Eady (1949) paper, and uses this to compute y-derivatives when necessary. In both cases the problem becomes two-dimensional.

Set $\theta = \beta = \bar{q}_y = 0$, so that the vertical density gradient $-\Delta\rho/H$ is uniform, and the horizontal density gradient is also uniform and directed in the y-direction, of size $f\rho_0\bar{u}_z/g$ from thermal wind, where $\bar{u}_z$ is constant. For convenience, we nondimensionalise the problem. Scaling z on H, ρ on

$\rho_0 g' H$, where $g' = g\Delta\rho/\rho_0$, mean flow $\bar{u} = \bar{z}\bar{u}_z$ on $\sigma g' H/fL$, where L is again the horizontal scale of the mean flow and σ is the ratio of the horizontal to the vertical variation in mean density, k on a^{-1}, where a is the deformation radius $(g'H)^{1/2}/f$, gives the familiar equation for the perturbation pressure as

$$p_{zz} = k^2 p, \quad p = \gamma(\cosh kz + iA \sinh kz) \tag{6.1}$$

where γ is the (small) amplitude of the solution.[7] Here, for convenience, the surface and floor are at $z = \pm 1/2$. We denote $|\gamma|^2$ by G [which is thus O(a^2) in earlier notation]. In the wide case, G would usually be independent of y for most extant parameterisations; each value of y would look similar. In the case when channel walls are important (i.e., the original Eady problem), G would take the form $\cos^2 \pi y$ if the channel lies between $y = \pm 1/2$, so that there is no perturbation at the vertical walls.

Applying the boundary conditions ($w = 0$ at surface and floor) gives the standard results that

$$iA = \frac{1}{2c}\left(\tanh\frac{k}{2} - \frac{2}{k}\right) \tag{6.2}$$

Then

$$c^2 = -\frac{1}{4}\left(\tanh\frac{k}{2} - \frac{2}{k}\right)\left(\frac{2}{k} - \coth\frac{k}{2}\right) \tag{6.3}$$

is the purely imaginary phase velocity. For the fastest growing mode,

$$k = 1.6062, \ A = 1.5018, \ c_i = 0.1929. \tag{6.4}$$

We now compute all relevant quantities. We have

$$c = ic_i$$

$$v' = ikp, \ u' = 0, \ \rho' = -p_z, \ w' = ik\sigma(p - (z - c)p_z) \tag{6.5}$$

so

$$\overline{v'\rho'} = \frac{1}{2}\,\mathrm{Re}(ikp \cdot -p_z^*) = -\frac{k^2 GA}{2} \tag{6.6}$$

which is independent of z.

---

[7] The formulation in density co-ordinates looks almost identical, with the replacement of z by $-p$ and of p by the Bernoulli function $B = p + \rho gz$. Interpretations of various quantities, of course, differ intrinsically. Near the surface, quantities vary sinusoidally and the simple example in Fig. 2 is an approximate representation of the problem.

Next,

$$\overline{w'\rho'} = \frac{k\sigma}{2}\,\mathrm{Re}(i[p - (z - c)p_z] \cdot -p_z^*)$$
$$= \frac{k^2\sigma G}{2}\{kc_i(\sinh^2 kz + A^2 \cosh^2 kz) - A\} \tag{6.7}$$

whose terms are familiar from before. This, of course, vanishes at surface and floor from the boundary condition.

Thus

$$\overline{(v'\rho')_y} = -\frac{k^2 A}{2}G_y \tag{6.8}$$

$$\overline{(w'\rho')_z} = \sigma k^4 c_i(1 + A^2)G \sinh kz \cosh kz \tag{6.9}$$

so that the eddy density flux terms are

$$\nabla \cdot (\overline{\mathbf{u}'\rho'}) = -\frac{k^2 A}{2}G_y + \sigma k^4 c_i(1 + A^2)G \sinh kz \cosh kz. \tag{6.10}$$

In the quasi-geostrophic limit when σ is small, the $\overline{w'\rho'}$ term is negligible and only cross-stream variations in amplitude generate changes in the mean density. However, in the planetary geostrophic regime, the mean density can also change because of the (ageostrophic) vertical velocity.

We can also compute the terms in the TRM formulation away from the horizontal boundary layers. Here, the second term has no effect (it is oriented in the $x - z$ plane only). The remaining term is simply

$$\psi_2 = \frac{\overline{v'\rho'}}{\bar{\rho}_z} = \frac{\overline{v'\rho'}}{\overline{v'\rho'}} = -\frac{k^2 AG}{2}. \tag{6.11}$$

which is uniform in z. Thus

$$v^+ = \frac{\overline{v'\rho'}}{\bar{\rho}_z} = \psi_{2z} = 0 \tag{6.12}$$

for this case. (Indeed, in density co-ordinates, $\overline{v'h'} = 0$ identically.) The pseudo-vertical velocity is

$$w^+ = -\psi_{2y} = \frac{k^2 A}{2}G_y \tag{6.13}$$

and the pseudo-vertical flux is

We now consider the temporal change terms. From M, these are given by (2.1) to (2.3); substitution gives

$$(w^+\bar\rho)_z = w\,\bar\rho_z = -w^+ = -\frac{k^2A}{2}G_y.$$ (6.14)

which is of second order compared with $\bar\rho$, so that gradients of $\bar\rho$ are also those of $\tilde\rho$. However,

$$\hat\rho = \frac{1}{2}\sigma k^3 G(1+A^2)\sinh kz \cosh kz$$

which is *not* small compared with $\bar\rho$, but the same (2nd) order.

If the effect of eddies is presented as an eddy flux divergence, then we have (respectively)

$$\hat\rho = 2kc_i\hat\rho = \sigma k c_i(1+A^2)G \sinh kz \cosh kz$$ (6.15)

If the effect of eddies is presented using a quasi-Stokes streamfunction, then (respectively)

$$\bar\rho_t + \nabla \cdot (\mathbf{u}^+\bar\rho) = \bar\rho + \hat\rho_t + \nabla \cdot (\overline{\mathbf{u}^+\rho}) = 0, \text{ i.e.}$$ (6.16)

$$\bar\rho_t + \nabla \cdot (\mathbf{u}^+\bar\rho) = 0, \text{ i.e.,}$$

$$\bar\rho_t - \frac{k^2A}{2}G_y = \bar\rho_t + \sigma k^4 c_i(1+A^2)G \sinh kz \cosh kz = 0.$$

$$\tilde\rho - \frac{k^2A}{2}G_y = \rho_t + \sigma k^4 c_i(1+A^2)G \sinh kz \cosh kz - \frac{k^2A}{2}G_y = 0.$$ (6.17)

Both expressions are identical, as they must be.[8] The two formulations look very different. Suppose the y-variation of the perturbation is weak. Then in the Eulerian interpretation, the hyperbolic function term gives a decrease in $\bar\rho$ near-surface and an increase at depth. In the MMD formulation, there is no change to interior mean density at all (the changes are confined to the boundary layers discussed previously). The effect of the remaining term is uniform in depth, and gives (usually) an increase in density at the southern (light) side of the channel and a decrease at the northern (heavy) side in both formulations. Fig. 4 shows how these quantities vary in the vertical.

We consider two possibilities in turn, which will demonstrate *inter alia* a shortcoming in locally-based eddy parameterisations.

---
8 In the quasi-geostrophic limit, only the term in G_y survives.

(a) *the eddies have the same amplitude at all points*

A local parameterisation would assume the eddies to have the same amplitude at each point across the channel (alternatively, we can imagine the solution when the channel width becomes asymptotically large and the cross-channel variation becomes small). Then the interior quasi-Stokes velocity is everywhere zero, and changes in density structure are solely produced by the M correction to the density trend. This is perhaps not a particularly helpful interpretation, since we feel intuitively that the density *does* change in the Eady problem due to the slumping induced by release of A.P.E. as the eddies grow. If our model density field is taken to represent $\tilde\rho$, then it will not change in the interior until the eddies become nonlinear (beyond the scope of the discussion).

Most parameterisations in this case yield a uniform (negative) value for the quasi-Stokes streamfunction in the ocean interior, and so – correctly – no cross-channel TRM flow there. The streamfunction must be set to zero on all boundaries. The vertical wall conditions yield, as in Fig. 5, a flow which contains two delta-functions in w^+, with rising fluid at the warm wall and sinking fluid at the cold wall. These two circulations – which, as we have seen, are not present in the Eady solution – will act to initiate a slumping of the fluid. Once this slumping begins, the problem ceases to be purely Eady-like, and so is more complicated. Nonetheless, the behaviour is *not* that observed in the Eady solution near the vertical walls, but is acceptable for the EMD interpretation near the horizontal surfaces.

Setting ψ_2 to zero at the surface and floor creates additional delta-function fluxes horizontally which further aid the slumping process.

(b) *the eddy amplitude varies across the channel*

In the actual Eady problem, the amplitude varies across the channel. In such a case, v^+ remains zero, but w^+ is nonzero in both the interior and at surface and floor. Its pseudo-advection of mean density contributes part of the change in density, with the M term contributing the remainder.

The solution here is indicated in Fig. 6. Here we assume that the amplitude G increases monotonically from zero at the southern boundary to a maximum in the centre of the channel, and then decreases to zero again. The change in $\bar\rho$ is induced by a quasi-Stokes velocity which upwells

in the southern (light) half and downwells in the northern (dense) half of the channel, and delta-functions in quasi-Stokes horizontal velocity at surface and floor.

No locally-based parameterisation produces the behaviour in (b), preferring instead that in (a), showing that a fuller representation of eddy effects will have to take nonlocal factors into account.

7. Interactions between the two interpretations of density

We now return to the behaviour of the system with the two possible definitions of density. Formally, there are only two approaches: to use EMD, with the eddy terms being $\nabla \cdot (\overline{\mathbf{u'}\rho'})$; and to use MMD, with the quasi-Stokes streamfunction evaluated correctly everywhere. However, since the M formulae have been used in the earlier cited calculations as if they held everywhere, we shall note how these formulae produce incorrect values if applied unwisely.

We consider first the change in the area-integrated density field in a channel geometry for linear theory. Now this must be *zero*: integrating (1.2) across the channel area means that the divergences $(\overline{v'\rho'})_y$ and $(\overline{w'\rho'})_z$ both integrate to zero. Thus using an Eulerian mean,

$$\frac{\partial}{\partial t}\int \bar{\rho}\, dA = 0 \qquad (7.1)$$

where dA represents an infinitesimal area $dydz$, so that no mass can be gained or lost from the system. We have seen that the column integral of the MMD $\tilde{\rho}$ is identical, so that (7.1) must hold for accurately evaluated MMD. This is also clear from integrating (1.4) across the domain and from top to bottom:

$$\frac{\partial}{\partial t}\int \tilde{\rho}\, dA = 0 \qquad (7.2)$$

since the quasi-Stokes streamfunction is zero on all boundaries. However, (7.2) does not hold if the interior (M) formulation is used throughout the water column since the integral of density omits the surface and floor contributions which are second order in amplitude (being of magnitude α and of depth range α) and so contribute to the same order as the interior differences. Thus computations made with the interior formulations cannot be consistent. Mass conservation can only then be achieved by requiring ψ_2 not to vanish at surface and floor.

Calculations can also be made for the rate of change of potential energy PE. Appendix B shows that small-amplitude theory correctly conserves energy, so that $PE_t + KE_t = 0$. Both KE and PE have well-defined interpretations, furthermore, as being rates of change of some integral over a volume. Using the MMD formulation, KE_t should be identical, since evaluation of kinetic energy changes under either density interpretation involves an integration over the fluid column of the square of the amplitude of the fluctuations, and so further differences are at higher order, as are differences in the boundary layer near horizontal boundaries. If KE_t is the same for either definition of mean density, then PE_t should take the same value also.

Now PE losses are $O(\sigma)$ smaller than might be expected from scaling arguments, because horizontal fluxes $[\nabla_H \cdot (\overline{\mathbf{u}_H'\rho'})$ in the divergence form, $\nabla_H \cdot (\mathbf{u}_H^+\bar{\rho})$ in the TRM form] do not contribute to changes in PE (as can be seen after an integration by parts in the horizontal directions of the PE tendency terms). Only vertical (or pseudo-vertical) terms are left, plus terms in $\hat{\rho}$ in the TRM form.

For the Eady problem, we can compute potential energy changes directly. For the Eulerian case,

$$PE_t = \int \bar{\rho}_t\, dy\, dz \qquad (7.3)$$

nondimensionally. Integration across-channel eliminates the horizontal divergence in (6.16), so that only the vertical flux alters the PE, which from (6.9) is

$$PE_t = -k^4\sigma c_i(1 + A^2)\left\{\int G\, dy\right\}\int_{-1/2}^{1/2} z \sinh kz \cosh kz\, dz$$

so that

$$PE_t = -0.718\sigma \int G\, dy$$

for the fastest growing mode. Hence PE_t is negative, corresponding to a release of energy to perturbation kinetic energy KE (dominated by the v terms), since in this nondimensionalisation

$$KE_t = 2kc_i \cdot \frac{1}{2}\rho_0 \int (\overline{v'^2})dz = \frac{k^3\sigma c_i \int G\, dy}{2}\int_{-1/2}^{1/2} |p|^2\, dz = +0.718\sigma \int G\, dy = -PE_t$$

This balance, as noted, holds in general (see Appendix B).

Now we compute the equivalent using MMD. Again, this only yields sensible values if the exact

formulae are used everywhere. We do not know how to do this calculation directly, but the contributions from within the boundary layers are small compared with the answer, although the fact that there are rapid changes near the boundaries is vital to obtaining a non-zero answer. We have

$$\int z\tilde{p}_t \, dA = -\int z[\overline{(v^+\tilde{p})_y} + \overline{(w^+\tilde{p})_z}] \, dz \, dy = \int z(\psi_{2y}\tilde{p})_z \, dy \, dz =$$

$$-\int z(\sigma\psi_2)_z \, dy \, dz = -\sigma\int z\psi_{2z} \, dy \, dz = \sigma\int\psi_2 \, dy \, dz$$

$$= -1.94\sigma\int G \, dy.$$

The difference between the −1.94 and −0.718 values is precisely equal to the rate of change of *PE* computed using small perturbation Eady theory in density co-ordinates:

$$-\int z_{zz} \, dy \, dp = -1.22\sigma\int G \, dy, \qquad (7.4)$$

although this will not be pursued further. So estimates of *PE* changes using MMD are larger in magnitude (in this case) than their Eulerian equivalent.

We have already seen that the potential energy is not computed accurately within the MMD formulation; thus the time rate of change is also found inaccurately, and the energetics of the MMD average remain inconsistent.

8. Experiments with channel models

The arguments in the previous sections are partly generic and partly specifically based on linear theory. This section examines solutions to two-dimensional emulations of the three-dimensional channel model of Killworth (1998), using a variety of formulations to represent the eddy terms, specifically to examine boundary conditions and interpretations. One example, with different physics, was given earlier (Fig. 3).

Briefly, the model covered a longitude range of 2.6°, a latitude range of 5.2°, centred on 30°N, and a shallow depth of 300 m. The grid spacings were 0.02° east-west, 0.018° north-south (these were incorrectly stated to be 10 times larger in Killworth 1998 and 20 m vertically, with

viscosities 50 m² s⁻¹ (horizontal) and 5 × 10⁻⁴ vertically and diffusivities 10 m² s⁻¹ horizontally and 10⁻⁴ vertically. The vertical diffusivity was somewhat too large; analysis of the two-dimensional results below shows that vertical diffusion plays an important role in the temperature balance.

Starting from a narrow temperature front with uniform salinity, relaxation towards the initial temperature values in bands at north and south of the channel provided a source of potential energy. This method has the advantage that there are no regions of unstable or neutral stratification, thus avoiding difficulties about parameterisations in such regions. Averages were computed over time and longitude over 7.25 years between days 300 and 2950. For temperature and velocity these were computed on constant depth surfaces; for the eddy terms, on density (here temperature) surfaces. This choice of parameters was partly historical, and partly to avoid a nearly quasi-geostrophic situation, in which (for example) the Gent and McWilliams parameterisation reduces to constant lateral diffusion plus two delta functions at top and bottom.

Two-dimensional (latitude-depth) simulations were then run on a Cartesian grid, as described below, and the 4000-day computations (steady in almost all cases) compared with the averages from the three-dimensional run. Comparisons were made with the temperature field as a function of y (north) and z, and with the baroclinic u velocity.[9] The comparisons are not ideal. Like other published work, they are of Eulerian means only, and over a period probably an order of magnitude too short for a good statistical comparison. (However, the fields in Fig. 3 were visually unaltered by averaging over another period of similar length, so the statistics may be better than we suggest.) Comparisons can not sensibly be made with two-dimensional calculations over the same time span, since the intermediate time behaviour of the full eddying simulation and the two-dimensional calculations is invariably different. Thus only steady state two-dimensional results can be compared with the long-time average. The comparisons are shown in Table 1, and used both a direct correlation between the fields, which is of little discriminatory use, and a more stringent measure of explained variance due to Visbeck et al. (1997), namely

---

[9] As discussed by Killworth (1998), the two-dimensional runs have no depth-averaged u field, so that only the baroclinic u can be compared. The barotropic u field, as noted by Killworth, plays a not inconsiderable role in the dynamics.

$$C = 1 - \frac{\sum_{y,z} (\tau_2 - \tau_3)^2}{\sum_{y,z} (\tau_3 - \bar{\tau}_3)^2}$$

where τ represents either temperature or zonal velocity, the suffix whether a 2- or 3-dimensional field is considered (the 3-dimensional field being the zonal and time average above), and the bar representing a horizontal average. In practice, additional discriminatory power is gained by examining only the u measure, since to a large extent the temperature fields are constrained by the relaxation conditions. Both measures exclude the forcing region. Both integration time and the area for averaging have been modified since Killworth (1998). No parameterisation reproduced the 'pushing forward' of isopycnals in the MMD, so that direct comparisons with it are not useful.

Calculations were made using a variety of two-dimensional parameterisations, all written as divergences numerically (an alternative would be to use the skew-symmetric tensor formulation, cf. Griffies 1998), which are to be compared with the averaged three-dimensional solution. Fig. 7a shows the three-dimensional solution. To provide a yardstick for the various parameterisations, Fig. 7b shows the two-dimensional temperature field using only advection by the actual velocity fields plus the horizontal and vertical diffusivities used in the three-dimensional calculation. The solution is radically different, with the stratification almost vanishing in the interior of the channel. The imposed vanishing of the vertical temperature gradient at surface and floor). A better yardstick (Fig. 7c) is the same diffusive calculation, but using a horizontal diffusivity of 200 m² s⁻¹, which clearly gives results very close to the three-dimensional results.

The other parameterisations used were (in order of appearance in Fig. 7):

1 GM90 (Gent and McWilliams 1990, which has a constant diffusivity); Fig. 7d

2 K97 (more properly, the depth co-ordinate version of Killworth, 1997, discussed earlier, which computes a variable diffusivity); Fig. 7e

3 GMs (Gent and McWilliams 1990, but with the streamfunction non-zero at the surface); Fig. 7f

4 Ks (Killworth 1997, adapted as discussed below); Fig. 7g

5 VP (computing $(v'\overline{\rho})_y$ directly from small-amplitude formulae, also discussed below);

Fig. 7h

6 VPWP (computing $(v'\overline{\rho})_y + (w'\overline{\rho})_z$ directly from small-amplitude formulae, also discussed below); Fig. 7i

Before discussing the results, we briefly examine the rationales for the choices of parameterisations. The first two are straightforward. The GM parameterisation defines a streamfunction and deduces v^+ and w^+ therefrom, using $\psi_2 = \kappa \rho_y / \rho_z$, with $\psi_2 = 0$ at surface and floor; the delta-function changes are thus spread across the (relatively wide) top and bottom grid points. The diffusivity κ is taken as a constant. The K97 parameterisation is as discussed earlier, handling the delta-functions numerically as in Killworth (1998).

The third parameterisation, GMs, attempts to emulate a nonzero value of streamfunction at surface and floor. This is not an easy task numerically, since many apparently straightforward approaches generated numerical instabilities. These included extrapolation of either the isopycnic slope or the streamfunction to the boundary, and computation of boundary values using one-sided interpolation formulae. A slightly unsatisfactory approach which set the streamfunction at surface (floor) to the values immediately below (above) was eventually used; the disadvantage being that the v^+ field vanished in the top and bottom grid points.

The fourth parameterisation, Ks, attempted to do the same thing for K97, which only specifies v^+ but not w^+. The small-amplitude theory was used to define ψ_2 directly at surface and floor from (3.19), and then v^+ [given by (3.14)] is integrated w.r.t. depth to obtain the streamfunction everywhere. No stable scheme was found when Killworth's (1997) parameter A became larger than about 6, which was needed for a reasonably accurate representation of the three-dimensional fields.

The last two parameterisations, for the EMD, directly evaluate either $(v'\overline{\rho})_y$ or $(v'\overline{\rho})_y + (w'\overline{\rho})_z$ directly from small-amplitude theory, again using Killworth's (1997) scalings. Neither calculation requires unknown boundary conditions. Under quasi-geostrophic circumstances, both parameterisations would be identical, but in the channel model run here this is not necessarily so. The former could contain some measure of the rotational flux, though the latter could not, apart from numerical approximations. Note that direct attempts to parameterise the flux divergence

usually suffer from Veronis effects (Veronis, 1975); however, this approach does not, since the terms are derived from solutions to the equations of motion and so have the same conservation properties (for the flux terms) as the original system.

Table 1 shows the measures of fit for the solutions for each parameterisation, with the coefficient (diffusivity κ for Gent-McWilliams, the scaling factor A for Killworth) adjusted to values which generate the best fit. Usually not all four fits can be optimised simultaneously, and the values cited are slightly subjective (small changes affecting the second significant figure).

The most accurate version of the GM90 parameterisation for this problem has a κ of 160 m² s⁻¹, a little lower than that cited in Killworth (1998). The results for the GM90 (Fig. 7d) are very similar to those of pure diffusion (6c), although slightly less accurate than this in the u field. The similarity is surprising since the GM90 includes the strong northward (southward) advection near the surface (floor) which is not present in the simple diffusive case.

The most accurate version of the K97 parameterisation (Fig. 7e) has $A = 3$, as used in Killworth (1998) for the same problem. As Fig. 7e shows, this parameterisation is the only one to produce the 'doming' of the 15.5° isotherm near the northern boundary with any accuracy. It is, as Table 1 shows, the most accurate of the parameterisations.

If w^+ is not required to vanish at surface and floor, then for this geometry the parameter values used hitherto are insufficient to reproduce the three-dimensional solution. This is because the high northward advection near-surface is now lacking. For the GM90 parameterisation (Fig. 7f), κ needed to be increased an order of magnitude (to 1200 m² s⁻¹) in order to reproduce an approximation to the three-dimensional fields. Although the temperature field looks reasonable, the corresponding velocity is poorly reproduced, due to the strong surface front near the southern boundary. A similar finding holds for the K97 parameterisation (Fig. 7g; recall that this could not be run with a sufficiently high value of α for a proper parameterisation). Thus permitting non-zero w^+ at surface and floor has not achieved a higher accuracy than maintaining zero w^+, for this problem and choice of parameterisations.

However, the final two parameterisations (VP, VPWP) do not use the (ν^+, w^+) formulation, but

simply insert a parameterisation for mixing directly. The results (Figs. 7h, 7i) are very similar, with VPWP being slightly superior; both yield an accurate representation of the three-dimensional result.

In terms, then, of reproducing the *Eulerian* mean density, most schemes were successful, with the K97 and VPWP schemes marginally superior to the others, and schemes which permitted nonzero quasi-Stokes streamfunctions at the surface were quite inferior.

9. Discussion

This paper has examined two forms of mean density: Eulerian and modified, particularly with respect to the effects their adoption could have on the boundary conditions on parameterisations at surface and floor in practical applications.

We have shown that although the extant approximate formulae for the two mean densities suggest they are very similar (the M theory assumes small perturbations, as we do here), they differ an order of magnitude more strongly in a thin layer near surface (floor), within which much lighter (heavier) fluid occurs. This fluid represents the lighter (denser) fluid which is occasionally advected into the column by the eddies.

This paper has argued that within this narrow layer, quasi-Stokes streamfunctions, whether computed by inaccurate near-boundary second order formulae or exactly, possess a near-delta function behaviour, which can clearly not be well represented in numerical models. At finite amplitude, this layer would still be very thin and almost certainly unresolvable by most extant climate models. Thus it might well be that a better behaviour for parameterisations using the quasi-Stokes formulation would be to permit the streamfunction to be nonzero on surface and floor. Numerical experiments showed this not to be the case (the errors produced by nonzero surface streamfunctions were far larger than one would expect to be produced by the differences between definitions of mean density).

The remainder of the numerical tests showed that existing parameterisations, formally designed for MMD, proved capable of reproducing EMD well. In which case, does it matter which density

we interpret a mean as being? One test is to see whether a quasi-Stokes parameterisation, under steadily finer vertical resolution, can generate the additional boundary layer effects discussed at the start of this paper, which discriminate between the two densities much more strongly than interior changes. For finite amplitude eddies, the abnormal geometry used here implies a depth scale of about 50 m, so with adequate resolution, the differences between EMD and MMD should be resolvable. Accordingly, and for simplicity, a GM model was run, doubling vertical resolution several times, for the same time periods, requiring the streamfunction to ramp to zero only in the last gridpoint. There were no noticeable changes in density structure near the surface, suggesting that if we are to distinguish the two forms of density, quite a subtle parameterisation may be needed. Put another way, the parameterisations were reproducing the EMD, despite theory which suggests they should reproduce the MMD. It should be noted, of course, that the calculations were done with values tuned to fit the Eulerian mean, though wide investigations of parameter space yielded no solutions resembling the MMD.

Another result from the runs was that a direct parameterisation of the Eulerian mixing term $\nabla \cdot (\overline{\mathbf{u}'\rho'})$ appears to be highly accurate in reproducing the EMD, and avoids the Veronis effect which usually causes difficulties about direct parameterisations. This is in contrast to suggestions by M, who argued that parameterizing quasi-Stokes streamfunctions would be more straightforward than parameterizing mixing effects directly. Nonetheless, it should be remembered that the (marginally) most accurate parameterisation for this problem was the K97 formulation, which used a TRM formulation. Thus no unequivocal recommendation can be made regarding the form of parameterisations.

More direct comparisons clearly need to be made under a variety of forcings, geometry and parameter ranges; those of Treguier (1999) and Gille and Davis (1999) would make a useful start on the problem. These are solely two-dimensional, and gyre-scale computations using time as an averaging operator would give valuable three-dimensional information for this problem.

APPENDIX A: SCALINGS

The scalings should hold beyond the linear limit provided that the length scale remains the deformation radius. If the perturbation pressure is taken to be of order $\rho_0 g' H \gamma$, where γ is nondimensional, then from Section 3,

$$v' \sim \frac{g'H\gamma}{f_0\alpha}; \quad w' \sim \varepsilon\sigma\gamma Hf_0; \quad \rho' \sim \frac{\rho_0 g'\gamma}{g};$$

$$\overline{v'\rho'} \sim \frac{\rho_0 g'^2 H^2 G}{f_0\alpha g}; \quad \overline{w'\rho'} \sim \varepsilon\sigma \frac{H}{a}\frac{\rho_0 g'^2 HG}{f_0\alpha g}; \quad \frac{(\overline{v'\rho'})_y}{(\overline{w'\rho'})_z} \sim \frac{1}{\sigma};$$

$$\Psi \sim \frac{g'H^2 G}{f_0\alpha}; \quad \frac{\text{second term in } \Psi}{\text{first term in } \Psi} \sim \varepsilon\sigma$$

$$v^+ \sim \frac{g'HG}{f_0\alpha}; \quad w^+ \sim \varepsilon\frac{H}{a}\frac{g'HG}{f_0\alpha};$$

$$w^+\overline{\rho}_z^+ \sim \nabla_H \cdot (\overline{\mathbf{u}_H'\rho'}); \quad \frac{w^+\overline{\rho}_z^+}{v^+\overline{\rho}_y} \sim \frac{1}{\sigma};$$

$$\hat{\rho} \sim \frac{\rho_0 g'}{g}G; \quad \frac{\hat{\rho}}{\overline{\rho}_t} \sim \sigma.$$

where G represents $|\gamma|^2$.

This demonstrates Treguier *et al.*'s (1997) arguments for the quasigeostrophic regime. In such cases (small σ), $(\overline{v'\rho'})_y$ dominates over $(\overline{w'\rho'})_z$ by an amount σ^{-1}. However, in terms of TRM velocities, $w^+\overline{\rho}_z^+$ dominates over $v^+\overline{\rho}_y$ by the same amount. In other words, while we think of lateral TRM motions as relaxing some originally stratified front, in z-co-ordinates the relaxation is actually produced by pseudo-vertical motions. It is thus important that the pseudo-vertical motions are represented correctly in ocean model parameterisations.

Here we demonstrate that $(KE + PE)_t = 0$ for the linear theory here; I am not aware of any proofs beyond the quasigeostrophic regime. For simplicity, define again, following Killworth (1997),

$$\chi = \frac{p}{\bar{u} - c}. \qquad (B1)$$

Then the boundary conditions on χ are $\chi_z = 0$, $z = 0$, $-H$, and the governing equation becomes

$$\left[\frac{(\bar{u} - c)^2 \chi_z}{N^2}\right]_z + \left[\beta(\bar{u} - c) - \frac{k^2}{f_0^2}(\bar{u} - c)^2\right]\chi = 0. \qquad (B2)$$

Then we have, integrating only in the vertical,

$$KE_t = 2kc_i\rho_0 \int_{-H}^{0} \frac{1}{2}(u'^2 + v'^2)\,dz = \frac{k^3 c_i}{2f_0^2\rho_0}\int_{-H}^{0} dz\,|p|^2 = \frac{k^3 c_i}{2f_0^2\rho_0}\int_{-H}^{0} dz\,|\chi|^2\,|\bar{u} - c|^2. \qquad (B3)$$

Similarly, again integrating only in the vertical, noting that the horizontal divergences give no contribution when integrated across the domain,

$$PE_t = -g\int_{-H}^{0} z\,\overline{(w'\rho')}_z\,dz = g\int_{-H}^{0} \overline{w'\rho'}\,dz \qquad (B4)$$

where

$$w' = -\frac{ik}{\rho_0 N^2}(\bar{u} - c)\chi_z; \quad \rho' = -\frac{1}{g}\{(\bar{u} - c)\chi_z + \chi\bar{u}_z\}$$

so that

$$\overline{w'\rho'} = \frac{k}{2\rho_0 g}\operatorname{Re}\left[i\frac{(\bar{u} - c)\chi_z}{N^2}\left(\chi_z^*(\bar{u} - c^*) + \chi^*\bar{u}_z\right)\right].$$

Hence, noting the second bracket is an exact differential, and using (B2), we have

$$PE_t = \frac{k}{2\rho_0}\operatorname{Re}\left[i\int_{-H}^{0}\frac{(\bar{u} - c)^2 \chi_z}{N^2}\{(\bar{u} - c^*)\chi_z^*\}\,dz\right]$$

$$= \frac{k}{2\rho_0}\operatorname{Re}\left[i\int_{-H}^{0}\chi^*(\bar{u} - c)\left\{\beta(\bar{u} - c) - \frac{k^2}{f_0^2}(\bar{u} - c)^2\right\}\chi\,dz\right]$$

$$= \frac{k}{2\rho_0}\operatorname{Re}\left[i\int_{-H}^{0}dz\left\{\beta|\chi(\bar{u} - c)|^2 - \frac{k^2}{f_0^2}|\chi(\bar{u} - c)|^2(\bar{u} - c)\right\}\right]$$

after use of the boundary conditions. This can be further simplified to

$$= -\frac{k^3 c_i}{2f_0^2\rho_0}\int_{-H}^{0} dz\,|\chi|^2\,|\bar{u} - c|^2 = -KE_t \qquad (B6)$$

as required.

TABLE 1

Agreement measures for various two-dimensional parameterisations

Parameterisation	Value	T correlation	T explained	u correlation	u explained
Advection-diffusion	$\kappa = 10$ m² s⁻¹	0.80	0.99	0.81	-0.72
Advection-diffusion	$\kappa = 200$ m² s⁻¹	0.99	1.00	0.84	
GM90	$\kappa = 160$ m² s⁻¹	1.00	1.00	0.95	0.82
K97	$A = 3$	1.00	1.00	0.99	0.97
GMs	$\kappa = 1200$ m² s⁻¹	0.94	0.99	0.56	-1.46
Ks	$A = 5$; numerical difficulties for large A	0.91	0.99	0.84	0.16
VP	$A = 3$	0.99	1.00	0.96	0.84
VPWP	$A = 3$	0.99	1.00	0.97	0.87

References

Andrews, D. G., and M. E. McIntyre, 1976: Planetary waves in horizontal and vertical shear: the generalized Eliassen-Palm relation and the mean zonal acceleration. *J. Atmos. Sci.,* **33**, 2031-2048.

Bretherton, F. P., 1966: Critical layer instability in baroclinic flows. *Quart. J. R. Meteorol. Soc.,* **92**, 325-334.

de Szoeke, R. A., and A. F. Bennett, 1993: Microstructure fluxes across density surfaces. *J. Phys. Oceanogr.,* **23**, 2254-2264.

Eady, E. T., 1949: Long waves and cyclone waves. *Tellus,* **1**, 33-52.

Eby, M., and G. Holloway, 1994: Sensitivity of a large-scale ocean model to a parameterisation of topographic stress. *J. Phys. Oceanogr.,* **24**, 2577-2588.

Edmon, H. J., B. J. Hoskins, and M. E. McIntyre, 1980: Eliassen-Palm Cross Sections for the Troposphere. *J. Atmos. Sci.,* **37**, 2600-2616.

Gent, P. R., and J. C. McWilliams, 1990: Isopycnal Mixing in Ocean Circulation Models. *J. Phys. Oceanogr.,* **20**, 150-155.

Gent, P. R., J. Willebrand, T. J. McDougall, and J. C. McWilliams, 1995: Parameterizing Eddy-Induced Transports in Ocean Circulation Models. *J. Phys. Oceanogr.,* **25**, 463-474.

Gille, S. T., and R. E. Davis, 1999: The influence of mesoscale eddies on coarsely resolved density: An examination of subgrid-scale parameterisation. *J. Phys. Oceanogr.,* **29**, 1109-1123.

Greatbatch, R. J., 1998: Exploring the relationship between eddy-induced transport velocity, vertical momentum transfer, and the isopycnal flux of potential vorticity. *J. Phys. Oceanogr.,* **28**, 422-432.

Greatbatch, R. J., and K. G. Lamb, 1990: On Parameterizing Vertical Mixing of Momentum in Non-eddy Resolving Ocean Models. *J. Phys. Oceanogr.,* **20**, 1634-1637.

Green, J. S. A., 1970: Transfer properties of large scale eddies and the general circulation of the atmosphere. *Quart. J. R. Meteorol. Soc.,* **96**, 157-185.

Griffies, S. M., 1998: The Gent-McWilliams skew flux. *J. Phys. Oceanogr.,* **28**, 831-841.

Held, I. M., and T. Schneider, 1999: The surface branch of the zonally averaged mass transport circulation in the atmosphere. *J. Atmos. Sci.,* **56**, 1688-1697.

Killworth, P. D., 1997: On the parameterisation of eddy transfer. Part I: Theory. *J. Mar. Res.,* **55**, 1171-1197.

Killworth, P. D., 1998: On the parameterisation of eddy transfer. Part II: Tests with a channel model. *J. Mar. Res.,* **56**, 349-374.

McDougall, T. J., 1998: Three-dimensional residual mean theory. pp. 269-302 in: Ocean Modeling and parameterisation, eds. E. P. Chassignet and J. Verron. Kluwer, 451 pp.

McIntosh, P. C., and T. J. McDougall, 1996: Isopycnal averaging and the residual mean circulation. *J. Phys. Oceanogr.,* **26**, 1655-1660.

Merryfield, W. J., and G. Holloway, 1997: Topographic stress parameterisation in a quasi-geostrophic barotropic model. *J. Fluid Mech.,* **341**, 1-18.

Rix, N. H., and J. Willebrand, 1996: parameterisation of Mesoscale Eddies as Inferred from a High-Resolution Circulation Model. *J. Phys. Oceanogr.,* **26**, 2281-2285.

Robinson, A. R., and J. C. McWilliams, 1974: The baroclinic instability of the open ocean. *J. Phys. Oceanogr.,* **4**, 281-294.

Treguier, A. M., 1999: Evaluating eddy mixing coefficients from eddy-resolving ocean models: A case study. *J. Mar. Res.,* **57**, 89-108.

Treguier, A. M., I. M. Held, and V. D. Larichev, 1997: On the parameterisation of quasi-geostrophic eddies in primitive equation ocean models. *J. Phys. Oceanogr.,* **27**, 567-580.

Veronis, G., 1975: The role of models in tracer studies. *Numerical Models of the Ocean Circulation.* Natl. Acad. of Sci., 133-146.

Visbeck, M., J. Marshall, T. Haine, and M. Spall, 1997: On the specification of eddy transfer coefficients in coarse resolution ocean circulation models. *J. Phys. Oceanogr.,* **27**, 381-402.

Captions

1. (a) time variation of surface density (assumed sinusoidal). The shaded area shows densities which are lighter than the Eulerian mean $\bar\rho(0)$. (b) Any eddy transport in density layers in this range does not appear if the streamfunction is plotted against Eulerian mean density (i.e. the shaded area is lost) so that the streamfunction is nonzero at the 'surface' density. If plotted against modified density, streamfunction values are correctly recorded and the streamfunction becomes zero at the surface.

2. The differences between Eulerian mean and modified density. The upper diagram shows that the densities are very close to each other in the fluid interior (differing by O(α^2), where α is the small amplitude of the fluctuations). In a zone of size α near surface and floor, the two densities differ by a much larger amount, O(α), as indicated in the exploded lower view (which is actually the exact solution for sinusoidal time variation and uniform interior density gradient).

3. The Eulerian and modified mean density for a 4-year and along-channel average of an eddy-permitting channel model discussed in the text. (The average over the previous 4 year period is almost identical.) The problem was chosen to provide a larger vertical range over which the EMD and MMD differ than would hold for the real ocean, so that the vertical resolution (10 m) was adequate. Also shown is a typical two-dimensional parameterisation steady-state result, in this case following Gent and McWilliams (1990), using an eddy diffusion of 2000 m² s⁻¹. While the latter does not reproduce the EMD particularly well (true for a wide range of diffusivities), it does not reproduce the MMD at all where this differs from the EMD. This appears to hold for most extant parameterisations.

4. Tendency terms for the linear Eady problem. Shown are $\overline{v'\rho}$ (assumed independent of the cross-stream direction for simplicity), $\overline{w'\rho}$, and the resulting $\bar\rho_t$.

5. Schematic of the quasi-Stokes streamfunction generated from linear Eady theory for a very wide channel in which the eddy amplitude is the same at all points across the channel (as would be produced by most parameterisation schemes). No flow is generated save for two delta-function vertical velocities at the vertical walls, and two more, this time horizontal, at surface and floor.

6. The correct solution of the linear Eady problem's quasi-Stokes velocity when the eddy amplitude varies smoothly across the channel. Broad pseudo-vertical velocities w⁺ are produced with the signs as shown, acting to increase (decrease) the density of the light (heavy) water, and additional delta-function horizontal velocities induced by setting the quasi-Stokes streamfunction to zero at top and bottom.

7. Contours of temperature (°C; contour interval 0.5°C) and baroclinic u velocity (m s⁻¹; contour interval 0.004 m s⁻¹ with negative contours dashed) for (a) the time- and along-channel-averaged three-dimensional eddy-resolving calculation. The remaining panels are all for two-dimensional parameterisations. These are: (b) simple advection and diffusion using the values used in the three-dimensional calculation; (c) as (b), but with a horizontal diffusivity of 200 m² s⁻¹; (d) the Gent and McWilliams (1990) parameterisation, using κ = 160 m² s⁻¹; (e) the Killworth (1997) parameterisation using α = 3; (f) the Gent and McWilliams parameterisation modified so that the streamfunction does not vanish at surface or floor, using κ = 1200 m² s⁻¹; (g) the Killworth (1997) parameterisation, similarly modified, but for α = 5, which is too small to reproduce the three-dimensional calculation accurately due to numerical instabilities; (h) parameterizing simply $(\overline{v'\rho})_y$ directly from linear theory, with α = 3; (i) parameterizing $(\overline{v'\rho})_y + (\overline{w'\rho})_z$ directly from linear theory, with α = 3.
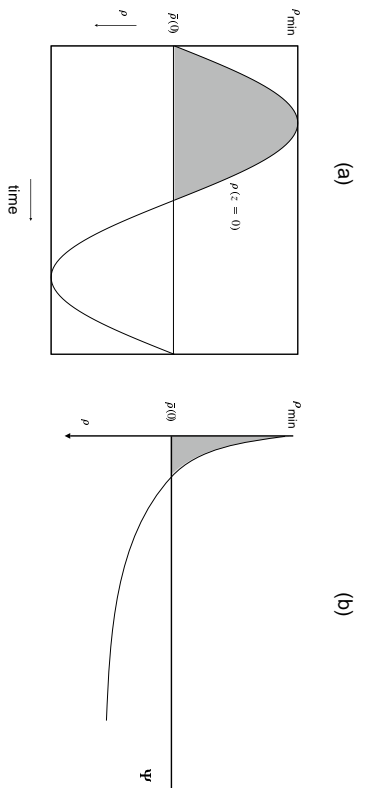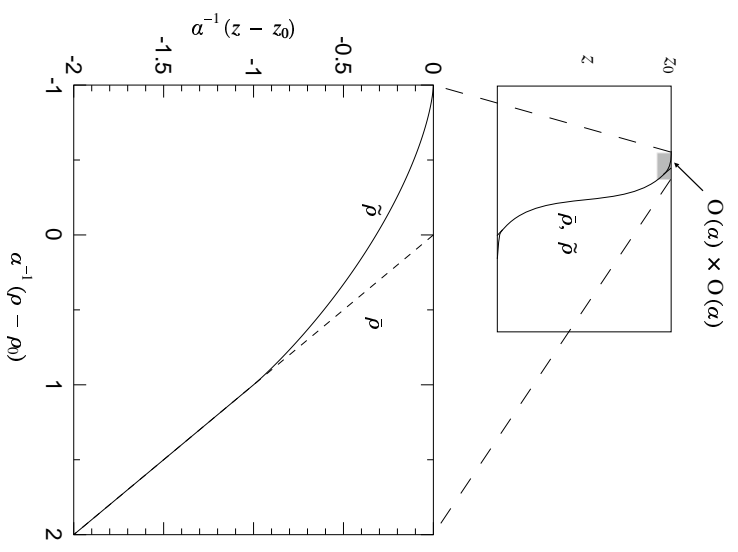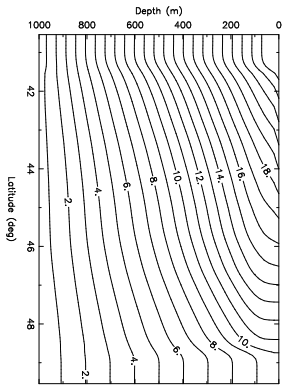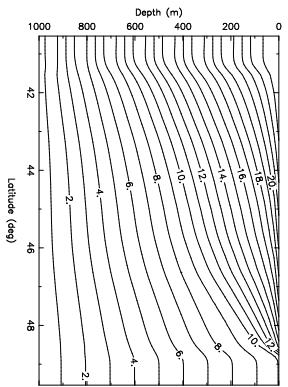
Figures

Figure 1

Fig. 2

Eulerian mean temperature

Modified mean temperature

GM90 mean temperature
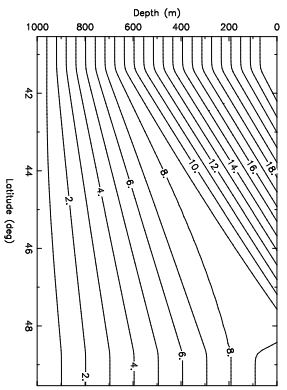
Fig. 3
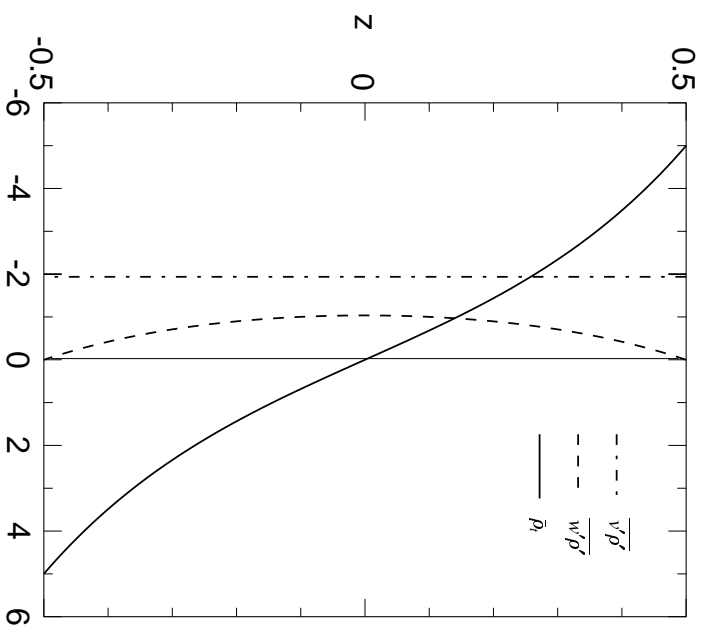
Fig. 4
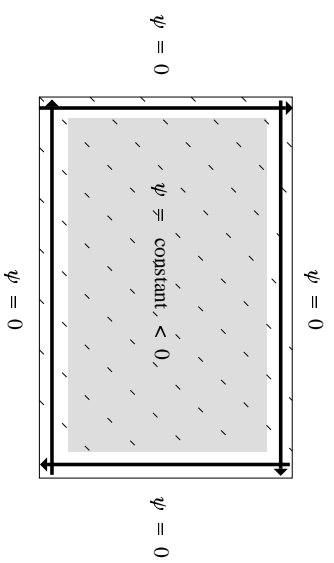
$\psi = 0$

$\psi = 0$

$\psi = 0$

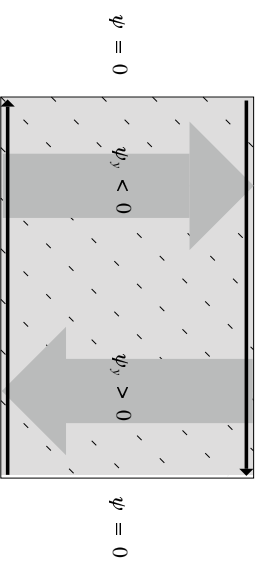$\psi = \text{constant}, < 0,$

$\psi = 0$

$\psi = 0$

Fig. 5

$\psi = 0$

$\psi_y < 0$

$\psi_y > 0$

$\psi = 0$

$\psi = 0$

Fig. 6

Temperature

Three-dimensional average fields

Baroclinic u velocity

(a)

(b)

Advection-diffusion (10 m^2 s^{-1})

(c)

Advection-diffusion (200 m^2 s^{-1})

Fig. 7a-c

Temperature

Baroclinic u velocity

GM90, $\kappa = 160 \ m^2 s^{-1}$

(d)

(e)

(f)
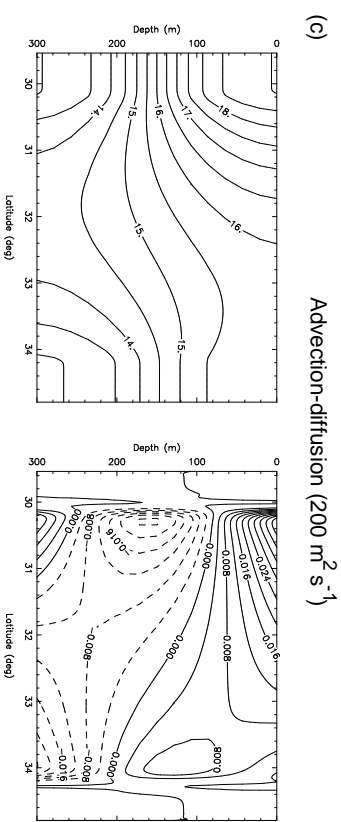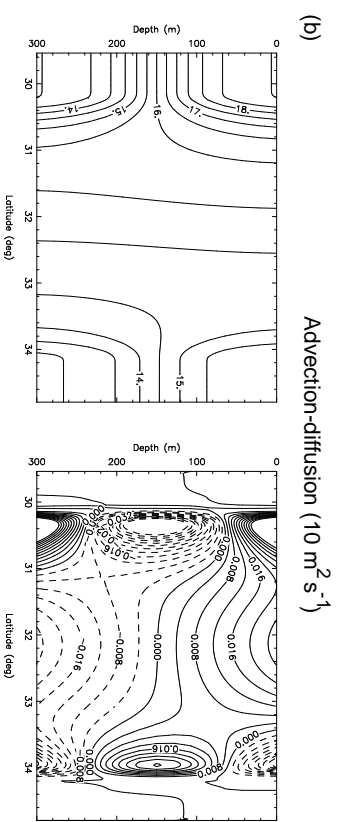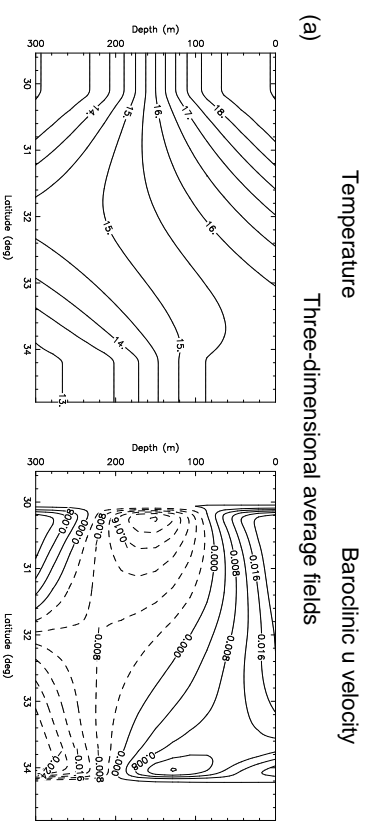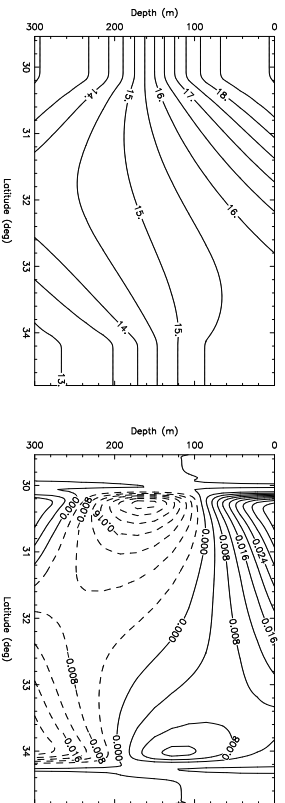
K97 ($\alpha = 3$)
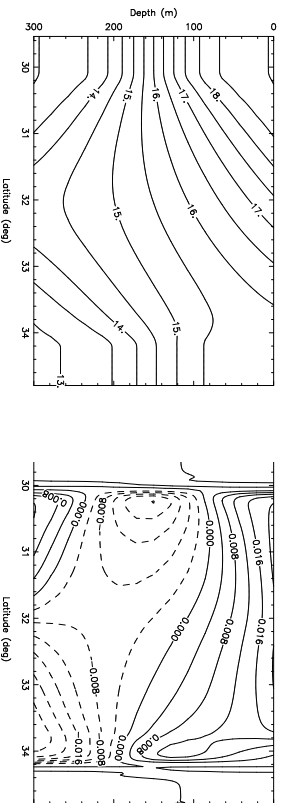
GM90, modified surface condition ($\kappa = 1200 \ m^2 s^{-1}$)

Fig 7d-f

27/7/00

Temperature

Baroclinic u velocity

K97, modified surface condition, $\alpha = 5$

(g)

(h)

(i)

VP, $\alpha = 3$

VPWP ($\alpha = 3$)

Fig 7g-i

27/7/00